ECMWF

European Centre for Medium-Range Weather Forecasts

Newsletter

No. 162 | Winter 2019/20

Forecasting Hurricane Lorenzo

Progress on cloud radar and lidar data

Checking Earth system observations

Global Flood Awareness System upgrade

Metview's Python interface

The hidden value of machine data

European Centre for Medium-Range Weather Forecasts, Shinfield Park, Reading, RG2 9AX, UK

Publication policy

The ECMWF Newsletter is published quarterly. Its purpose is to make users of ECMWF products, collaborators with ECMWF and the wider meteorological community aware of new developments at ECMWF and the use that can be made of ECMWF products. Most articles are prepared by staff at ECMWF, but articles are also welcome from people working elsewhere, especially those from Member States and Co-operating States. The ECMWF Newsletter is not peer-reviewed.

Any queries about the content or distribution of the ECMWF Newsletter should be sent to Georg.Lentze@ecmwf.int

Guidance about submitting an article is available at *www.ecmwf.int/en/about/media-centre/media-resources*

Investing in the future

ECMWF has signed a four-year contract with Atos for the supply of a new supercomputer to be installed later this year in our new data centre in Bologna, Italy. At over 80 million euros, this represents a big investment in European medium-range numerical weather prediction. The reason the Centre's Member States have given the green light is that we can only push the boundaries of predictability if we have the machines that can perform the required calculations. Numerical weather prediction needs supercomputers to estimate the current state of the Earth system and to evolve that state into the future using a sophisticated Earth system model. The finer the global grid on which the calculations are performed, the better the predictions can be. The new facility's additional computing power will be used to reduce the grid spacing for ensemble forecasts from 18 km today to about 10 km. It will also be used for investigative work towards the 5 km ensemble called for by ECMWF's Strategy to 2025, and to further develop the use of artificial intelligence in data assimilation and Earth system modelling.

It is not just raw computing power that matters: the code used for numerical weather prediction must be optimised to run as efficiently as possible on future high-performance computing facilities. ECMWF's Scalability Programme, a major programme to prepare all our systems for future supercomputer architectures, has yielded first results. They will enable efficiency gains by a factor of three on the new facility in Bologna. But work to ensure that the Centre's Integrated Forecasting System is fully open to upcoming technology solutions will continue. Several articles in this Newsletter illustrate recent progress. For example, steps are being taken to manage future growth in ECMWF's data archive, and close collaboration between researchers and computer scientists has enabled dramatic performance gains in the flood risk forecasts we produce for the EU's Copernicus Emergency Management Service.

Our high-performance computing facility serves not only to produce forecasts but also to run research experiments designed to push the boundaries of predictability. Examples presented in this Newsletter include ground-breaking work on the assimilation of cloud observations from satellite radar and lidar into ECMWF's Integrated Forecasting System, and progress towards assimilating satellite radiances in the visible part of the spectrum. The article on forecasting Hurricane Lorenzo shows some impressive predictions, but it also highlights some research questions that need to be addressed. The new supercomputer will enable us to make continued progress in research as well as operations to deliver more and better outputs for the benefit of our users in our Member States and beyond.

Florence Rabier
Director-General

Contents

Editorial
Investing in the future 1

News
Challenges in forecasting Hurricane Lorenzo 2
Cyclone Workshop showcases 3D visualisation. 4
Exploring online aircraft metadata 5
ECMWF signs contract for new supercomputer 6
Ocean5 charts made available online. 7
The 1994 Piedmont flood revisited. 8
Recent BUFR dropsonde data improved forecasts 9
Progress towards assimilating visible radiances 10
A heat health hazard index based on ECMWF data. 11
ECMWF's new IT network and security infrastructure in Bologna 12
Computing Representative meetings to become more interactive 13
Data archive growth: Escaping from the black hole. 14
GAIA 5.0: A science–art project using ECMWF data 15
New observations since October 2019. 15
EFAS upgrade improves performance and updates forecast products 16
ECMWF supports the South-East European Multi-Hazard Early Warning Advisory System 17
Users continue to rate Copernicus services highly 18
ERA5 reanalysis data available in Earth Engine 19

Meteorology
Progress towards assimilating cloud radar and lidar observations 20
Recent developments in the automatic checking of Earth system observations 27
New products for the Global Flood Awareness System. . . . 32

Computing
Metview's Python interface opens new possibilities 36
Unlocking the hidden value of machine data to improve ECMWF's services 40

General
ECMWF Council and its committees 44
ECMWF publications 45
ECMWF Calendar 2020 45
Contact information 46

Editor Georg Lentze • **Typesetting & Graphics** Anabel Bowen • **Cover** Wave height forecast and verification (see page 3)

Challenges in forecasting Hurricane Lorenzo

Linus Magnusson, Jean-Raymond Bidlot

The 2019 Atlantic hurricane season produced two Category 5 hurricanes on the Saffir–Simpson scale: Dorian and Lorenzo. Dorian formed south-east of Barbados on 24 August. It became a Category 5 storm before hitting the Bahamas, where it stalled and caused extensive damage. The cyclone then swept north along the US East Coast. Lorenzo formed on 23 September south of Cape Verde. It reached its maximum intensity on 29 September as the easternmost Atlantic Category 5 storm on record. The storm later weakened as it moved northward but caused problems on the Azores on 2 October, when the harbour on the Flores Island was severely damaged by high waves. Finally, the cyclone hit Ireland on 3 October as an extratropical system.

ECMWF's medium-range forecasts predicted Lorenzo's genesis much better than Dorian's, and early track forecasts gave a good indication of the cyclone's northward turn. However, the forecasts underestimated Lorenzo's propagation speed and there was great uncertainty in track forecasts as the storm approached Europe. Wave forecasts provided early indications of high waves around the Azores.

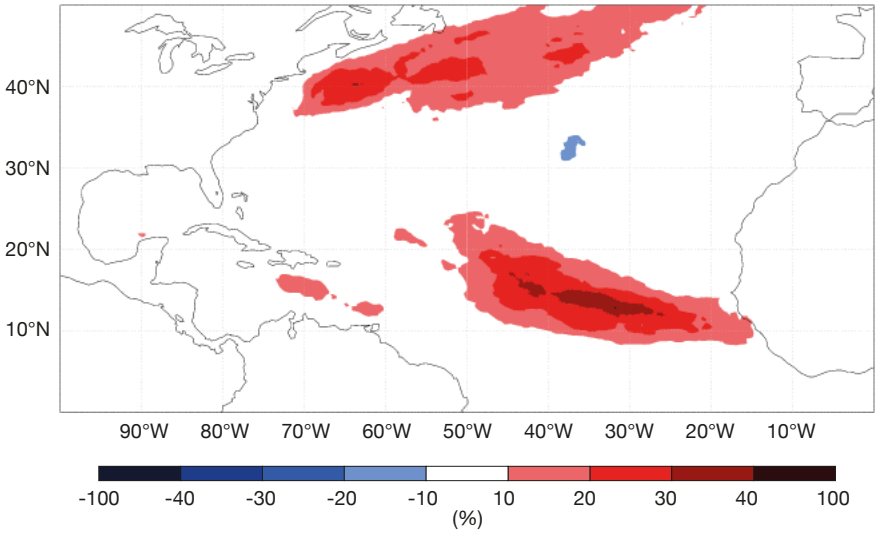

Weekly mean anomaly of tropical storm strike probability. The map shows tropical storm strike probability anomalies relative to the model climatology for 23 to 29 September in the forecast from 16 September 2019, i.e. one week before the formation of Lorenzo. The anomalies are calculated by subtracting the model climatological probabilities from the real-time forecast probabilities. Blue colours thus indicate a lower probability of tropical storm activity than in the 18-year climatology and red colours indicate a higher probability than in the climatology.

Genesis and track

As shown in the first figure, the genesis of Lorenzo was predicted by ECMWF ensemble forecasts exceptionally early. While the genesis of Lorenzo was predicted with high confidence more than a week in advance, ECMWF forecasts captured the genesis of Dorian only two days in advance. Big differences in predictability were also seen for major hurricanes in 2017. For example, the genesis of Irma was much more predictable than that of Harvey or Maria.

Ensemble forecasts for Lorenzo from before 22 September favoured a more westward track than the outcome. However, as illustrated in the second figure, the cyclone track forecast for Lorenzo from 24 September 00 UTC, issued just after the cyclone was classified as a tropical storm, already predicted a northward turn over the central Atlantic and provided an early indication that the storm might hit the Azores. However, comparing the position in the forecasts valid on 2 October with the observed position, we find that all members placed Lorenzo too far south, indicating a too slow propagation in all ensemble members.

In the ensemble forecast from 28 September, there was good agreement between all ensemble members on a path towards the western Azores. However, here too we find that in most ensemble members the propagation speed was too slow and the predicted position of Lorenzo on 2 October was too far south compared to the corresponding observation. The forecast from 28 September also missed Lorenzo's rapid intensification the following day (not shown).

After passing over the Azores, medium-range forecasts indicated large uncertainties in the path. In the forecast from 28 September 00 UTC, we find one group of members going towards the Bay of Biscay, another group towards Ireland and some members even further to the west over the central-northern Atlantic. This injected a lot of uncertainty into the forecast for western Europe at this point. The cyclone eventually hit Ireland as an extratropical cyclone on 3 October with strong winds.

Waves

During Lorenzo's passage over the Azores, waves were a major issue. The risk for extreme significant wave height south of the Azores between 1 and 3 October was picked up early in the forecast. As the bottom figure shows, as early as 25 October, i.e. a week in advance, the ensemble median was well outside the 99th percentile of the model climate distribution. Forecasts closer to the time predicted a significant wave height of around 14 metres (significant wave height roughly corresponds to the average height of the highest one third of waves). As shown in the figure, this corresponds well to altimeter satellite data available for about 04 UTC on 2 October close to the centre of the storm.

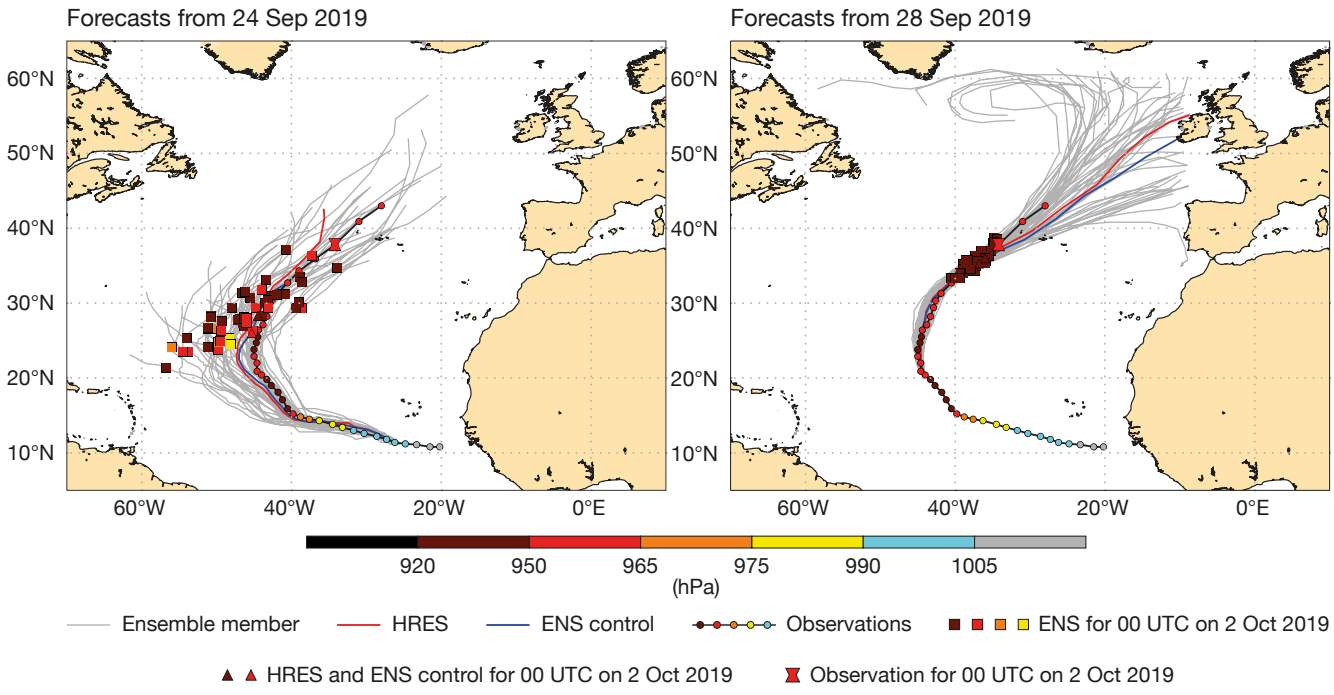

Track forecasts. The charts show tracks for tropical cyclone Lorenzo as predicted by individual ECMWF ensemble members, ECMWF's high-resolution forecast (HRES) and the ensemble forecast control member (ENS control) starting at 00 UTC on 24 September 2019 (top) and 00 UTC on 28 September (bottom). They also show best track observations at 6-hourly intervals and the predicted and observed position and intensity at 00 UTC on 2 October.

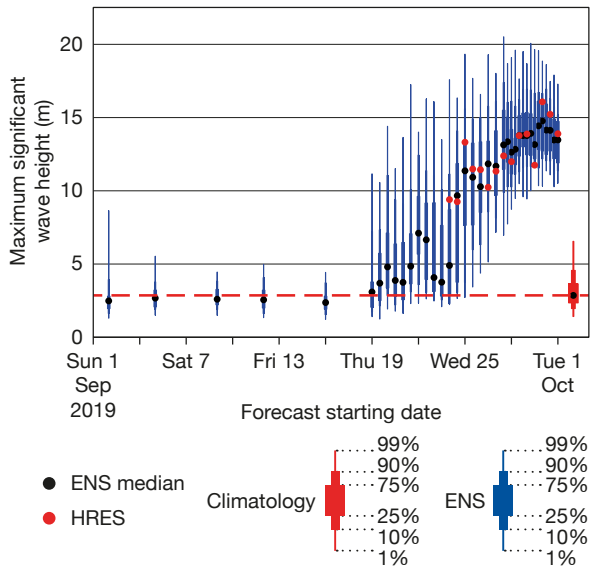

Ensemble wave forecasts. The chart shows the evolution of forecasts of maximum significant wave height for 1–3 October 2019 at 39°N, 31°W. The blue box-and-whisker symbols show ensemble forecasts (ENS) for different starting dates. The red dots indicate ECMWF's deterministic high-resolution forecasts (HRES).

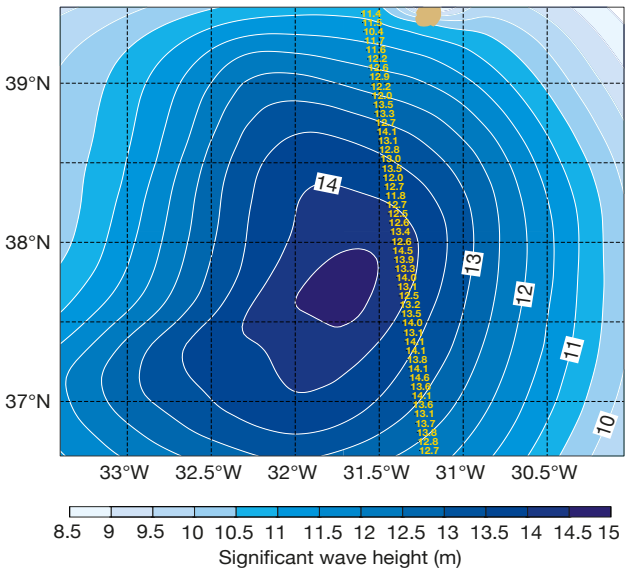

Wave height verification. The chart shows the high-resolution (HRES) significant wave height forecast starting at 00 UTC on 2 October 2019 and valid at 04 UTC overlaid with altimeter wave height data from CryoSat-2 (yellow numbers), which was over the area at about 04:17 UTC.

Discussion

The forecasts for Lorenzo exemplify several challenges. The excellent prediction of the genesis for Lorenzo contrasts with the much poorer forecast for Dorian. This raises the question of how the predictability of tropical cyclone genesis depends on the wider meteorological situation. Lorenzo's track was well predicted overall, but its predicted propagation speed was too slow compared to the observed speed, and forecasts missed a period of rapid intensification. These are issues which we have seen in several previous cases. Finally, Lorenzo injected a lot of uncertainty into forecasts for Europe during its extratropical transition. There are plans to study all these aspects of hurricane forecasting in greater detail in the coming years to enable us to further improve our medium-range predictions of tropical cyclones and the weather in Europe.

Cyclone Workshop showcases 3D visualisation

Marc Rautenhaus (Universität Hamburg), Tim Hewson (ECMWF), Andrea Lang (University at Albany)

The 19th Cyclone Workshop took place at Kloster Seeon in southern Germany from 29 September to 4 October 2019. The biennial workshop included a special two-hour session devoted to a '3D weather discussion'. The objective was to showcase recent advances in interactive 3D visualisation in the Met.3D package and to demonstrate how these can be used for rapid real-time analysis of ensemble forecasts. A team of three (this article's authors) led the proceedings and, with active participation from the audience, performed a real-time analysis of the then-current weather situation over the North Atlantic. We focused on the behaviour of Hurricane Lorenzo and its implications for the extratropical flow in ECMWF's ensemble forecasts.

The Met.3D software is an open-source package originating from visualisation research at Universität Hamburg and at Technische Universität München. From its original purpose of aiding forecast exploration during aircraft-based field campaigns (see ECMWF Newsletter No. 138), it has in recent years evolved into a general-purpose meteorological visualisation tool. In particular, through collaboration between Tim Hewson and the Met.3D group integrated into the German Collaborative Research Centre 'Waves to Weather' (W2W), novel feature-based displays for 3D jet-stream core lines and 3D frontal surfaces have been developed. Also, a user-friendly interface between ECMWF's Metview software and Met.3D has been created.

Visualising Lorenzo

Hurricane Lorenzo made its way through the eastern Atlantic Ocean in late September and early October and became the easternmost Category 5 hurricane on record in the Atlantic. During the period of the workshop, the storm underwent extratropical transition and curved back towards Europe. About 125 scientists from all over the world had assembled for this workshop to discuss the structure, dynamics, hazards, and predictability of extratropical and tropical cyclones, so this meteorological situation provided an ideal focal point for an interactive discussion of the ensemble forecast in real-time.

During the weather discussion, Met.3D was run remotely from the W2W visualisation server in Munich, although a standard PC equipped with a graphics card and data on disk would have worked equally well. We first introduced Met.3D's philosophy of building a bridge from traditional 2D visualisations (e.g. horizontal maps, vertical sections and Skew-T diagrams) that can be displayed and interactively moved in real time in a 3D context, to 'pure' 3D visualisations (including isosurfaces, direct volume rendering, trajectories and the novel jet-stream core line and frontal surface displays). Then, we used some standard Met.3D forecast products to obtain 'big picture' information on the weather situation. Afterwards, the audience could make special requests.

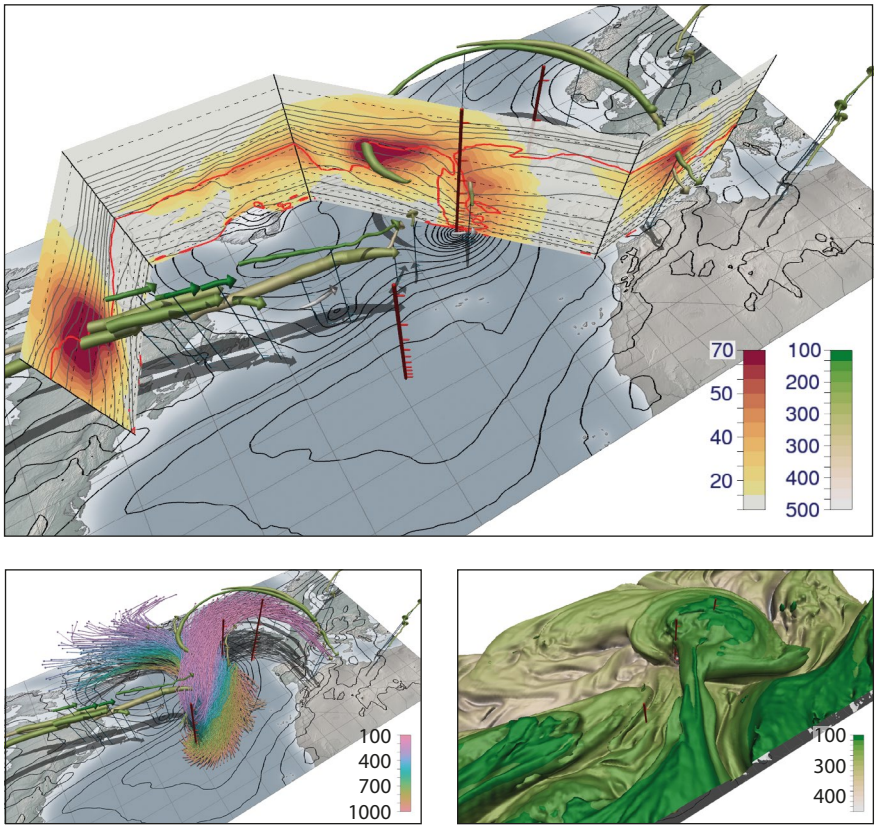

Examples of Met.3D visualisations used to analyse the behaviour of Hurricane Lorenzo. The panels show member 24 of the ECMWF ensemble forecast (ENS) from 00 UTC 29 September 2019, valid at 00 UTC 03 October 2019. Top: Jet-stream core lines where wind speed exceeds 45 m/s (colour shows pressure in hPa, thickness scaled according to wind speed), with vertical sections showing wind speed (colour in m/s), potential temperature (grey contours), and the 2-PVU line (red contour line) to indicate the dynamical tropopause (and a Lorenzo-related 'PV tower'). Black surface contours show mean sea level pressure. The three red vertical axes mark (from west to east) the centre of Lorenzo at 12 UTC 01 October 2019; the centre at 00 UTC 03 October 2019; the approximate location of maximum tropopause height as indicated by the 2-PVU isosurface. Bottom left: As top panel but with trajectories indicating warm conveyor belts (from 12 UTC 01 October 2019 until 00 UTC 03 October 2019, shown only where ascent is >500 hPa in 48 hours, colour shows pressure in hPa). Bottom right: 2-PVU isosurface representing the dynamic tropopause (colour shows pressure in hPa), with vertical axes as on the other panels.

Useful links

Met.3D website: *https://met3d.wavestoweather.de*

Met.3D publications: *https://met3d.wavestoweather.de/publications.html*

19th Cyclone Workshop: *https://www.wavestoweather.de/meetings/19th-cyclone-workshop/*

The figures show examples of visualisations used during the session. For instance, there was particular interest in the structure of the dynamical tropopause as represented by the 2-PVU isosurface, its relation to the jet-stream configuration, and trajectories carefully selected to represent warm conveyor belts (thanks to Julian Quinting from the Karlsruhe Institute of Technology for the trajectory data). A memorable moment occurred whilst interactively moving a vertical cross section during a phase of explosive extratropical re-intensification of Lorenzo, in one ensemble member. The descent of the 2-PVU isosurface to a level close to the surface near the cyclone led to great excitement in the audience! At the same time, the 3D jet lines were able to pick up cores at multiple levels, including the dynamical drivers at upper levels, and surface-wind-related cores at low levels.

Weather discussion with Met.3D. Andrea, Tim and Marc analysed ECMWF forecasts of Hurricane Lorenzo using interactive 3D visualisation whilst an active audience participated with ideas and suggestions for the forecast exploration.

Outlook

We are very encouraged by the positive feedback from the audience and look forward to the recently started second phase of W2W, in which Met.3D research and development will be actively continued. Jet and front diagnostics will be further improved, and we will evaluate a possible integration of the techniques into ECMWF's operational analysis toolchain in 2020.

Exploring online aircraft metadata

Bruce Ingleby (ECMWF), Mickey Yun Chan (Latvia University of Life Sciences and Technologies), Mohamed Dahoui (ECMWF)

ECMWF is working towards improving the use of meteorological observations from aircraft by adding information such as aircraft type and airline. A matching between meteorological observations and online data was achieved using a method developed as part of the ECMWF Summer of Weather Code programme (ESoWC 2019, see ECMWF Newsletter No. 161).

How it works

Biases in aircraft observations of temperature are known to depend on both aircraft type and airline, due to different avionics systems employed by the various airlines and aircraft fleets. In a few cases, different avionics can also result in gross errors in wind observations. The idea behind the method developed during ESoWC 2019 is to use aircraft type and airline metadata information available online to improve the assimilation and monitoring of aircraft weather reports.

ECMWF currently receives about 840,000 aircraft-based observations per day from around the world, most of which are AMDAR reports. The wind, temperature and (in some cases) humidity data provide valuable input to our forecasting system. When the main AMDAR programmes started several decades ago, the airlines and pilot associations insisted on anonymisation of aircraft identities. As a result, while each AMDAR report includes an 'identifier' unique to the aircraft which produced it, in most cases the type of aircraft and the airline cannot be deduced directly from the identifier. However, about 15 years ago online aircraft tracking systems started to provide information on flights using a mixture of crowdsourced radio messages and information from the airlines. The method developed during ESoWC 2019 matches aircraft metadata from those online resources to the aircraft identifiers included in AMDAR reports. Online data from the flightradar24 and flightaware websites essentially provide take-off and landing times and the airports involved for each aircraft. AMDAR reports are sorted by identifier and time, the first and last report in each flight are identified and the position is used to find the nearest likely airport. The two data sources are then matched together in order to link AMDAR aircraft identifiers with aircraft type and airline metadata. AMDAR reports from European and other airlines sometimes start and stop in mid-air, making the deduction of the airport where the aircraft came from or are flying to difficult or impossible. It is also more difficult where several airports are close together. A minority of AMDAR reports contain airport information, which makes matters easier. Despite the problems, useful progress has been made.

As an example, the figure shows schematically in black the movements of one aircraft over about six days, as available from flightradar24. This has been matched with the estimated movements of an aircraft associated with a particular AMDAR identifier. For non-US AMDARs, about half of the AMDAR identifiers have been matched with aircraft metadata in this way with

reasonable confidence. For the USA, the figure is about 15%. Interestingly, the South Korean AMDAR programme uses tail number as the AMDAR identifier, so all their AMDAR identifiers can easily be matched with aircraft type and airline.

Outlook

In view of the information available from flight tracking websites, the anonymisation of meteorological reports seems rather outdated. It may also make the forecasts available to airlines worse than if the metadata were available. While the matching process described above could be improved (and use of the OpenSky Network website investigated), a more long-term solution may be to engage in dialogue with the airlines to try to obtain the required metadata directly from them. The US National Oceanic and Atmospheric Administration (NOAA) and EUMETNET (a consortium of European national meteorological services) would also be involved. However, it is likely that this process will take some years.

In 2020, the World Meteorological Organization and the International Air Transport Association (IATA), an association of the world's airlines, are expected to start implementing a global AMDAR development programme (WICAP), which should boost airline participation and hence the number of AMDAR reports in the next few years. Another recent development is the use of air traffic management Mode-S reports to provide very high-density data (particularly winds) over parts of Europe and potentially elsewhere. Mode-S data are not yet processed at ECMWF, but in collaboration with EUMETNET and our Member States we are starting to plan the steps towards usage. These issues and others will be discussed at a workshop on Aircraft Weather Observations and their Use to be held on 12 and 13 February 2020, organised by EUMETNET and ECMWF. More details are available on the ECMWF website: https://www.ecmwf.int/en/learning/workshops/workshop-aircraft-weather-observations-and-their-use.

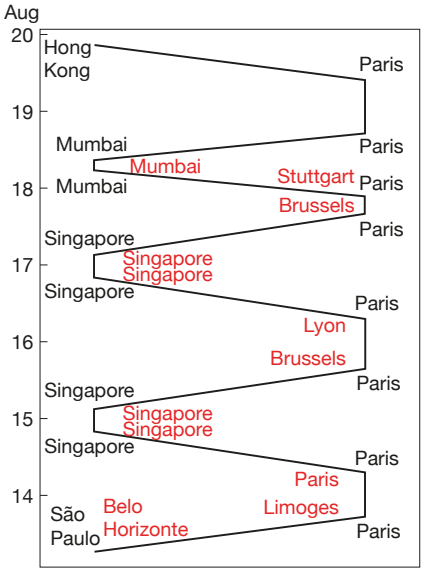

Identifying an aircraft from its movements. The figure shows the movements of an aircraft for about six days. The red writing shows estimated landings and take-offs according to time and location data included in AMDAR reports for a specific aircraft (AMDAR identifier EU1006). The method developed during ESoWC 2019 made it possible to match this estimated trajectory with online information (from the flightradar24.com website) on the trajectory of an Air France Boeing 777 (tail number F-GSQH), shown in black writing. The location discrepancies are a result of the fact that first/last AMDAR reports are not necessarily sent during ascents/descents but may be sent while the aircraft is closer to another airport, for example Belo Horizonte instead of São Paulo or Lyon/Brussels instead of Paris.

ECMWF signs contract for new supercomputer

ECMWF has signed a four-year contract worth over 80 million euros with Atos for the supply of its BullSequana XH2000 supercomputer. In December, ECMWF's Council of Member States had given the Centre the green light for the deal at the end of an international tender process in which bidders were assessed against criteria including committed performance, implementation plan, flexibility and risks, quality of technical solution, environmental impact, quality of service provision and support, and price.

The new system will deliver an increase in sustained performance by a factor of about five compared to ECMWF's current high-performance computing facility. This will enable advances such as increasing the ensemble forecast horizontal resolution from a grid spacing of 18 km to about 10 km, which is expected to significantly improve forecasts of near-surface temperatures and winds. The improved computing power will also make it possible to increase the ensemble forecast vertical resolution from 91 layers to 137 layers, in line with the current high-resolution forecast, and to issue extended-range forecasts daily rather than twice-weekly.

The increased capability will enable the Centre to continue investigative work towards the 5 km ensemble called for by its ten-year Strategy to 2025, and in the field of machine learning in numerical weather prediction. The Atos system will be hosted in the new ECMWF data centre currently being developed by the Italian Government and the Regione Emilia Romagna in Bologna, Italy. It is expected to be fitted in 2020 and to become fully operational in 2021.

Left. ECMWF's Council approved the deal in December 2019. **Right.** Senior Executive Vice-President Adrian Gregory, CEO UK&I, signed the contract for Atos and Director-General Florence Rabier signed it for ECMWF. (*Photo: Stephen Shepherd*)

Ocean5 charts made available online

Éric de Boisséson

Ocean5 is ECMWF's current ocean and sea-ice analysis system. It provides initial conditions for the ocean and sea-ice component of ECMWF's Earth system forecasting system. Ocean5 runs both a behind-real-time stream that produces the Ocean Re-Analysis System 5 (ORAS5) and a near-real-time (NRT) stream. ORAS5 is used for climate monitoring while Ocean5 NRT provides initial conditions for the Centre's forecasting activities. Charts for each stream are now freely accessible to both internal and external users on the ECMWF website. The case of the North Pacific 'Blob' discussed below illustrates how the charts can be used.

ORAS5 page

The ORAS5 web page targets users interested in climate monitoring. The charts on that page show monthly averages of ORAS5 with around a month and a half delay with respect to the current month. Three-month and yearly averages as well as 11-year and 21-year records are also shown. The full period (1979–now) of the reanalysis is covered for users interested in interannual to decadal climate variability. Ocean and sea-ice charts range from maps to vertical sections and time series. The different charts aim to complement each other. For example, the source of an anomaly in sea-surface temperature seen in the tropical Pacific can be tracked down by looking at the atmospheric fluxes received by the ocean, the vertical structure of the ocean and the magnitude of ocean transports. The anomaly can also be viewed in the context of the past months to decades and potentially linked to climate patterns, such as the El Niño Southern Oscillation (ENSO), a periodic warming and cooling of the equatorial Pacific Ocean.

Ocean5 NRT page

The Ocean5 NRT page is more limited. It provides daily maps of ocean and sea-ice parameters to provide an overview of the response of the ocean to current weather events, such as tropical cyclones, or to modes of variability, such as ENSO and the North Atlantic Oscillation. One-year long longitude–time diagrams at the equator are also available to monitor the evolution of the state of ENSO.

The North Pacific 'Blob'

From the implementation of the NRT Ocean5 monitoring page in early November 2019 to the time of writing (mid-December), the daily sea-surface temperature maps showed a persistent anomalously warm water mass off the west coast of North America and Alaska. This is illustrated in the figure for 26 November 2019. The climate community noticed these unusually warm sea-surface temperatures as early as the end of the summer. The generation of this 'marine heatwave' was favoured by an atmospheric blocking event allowing stronger than usual solar radiation to warm the north-east Pacific in August. The reason behind the scrutiny triggered by this event is its similarity with the long-lasting marine heatwave in the same area from 2014 to 2016, which was baptised 'the Blob' by the community. The 'Blob' formed under similar atmospheric conditions as this year's marine heatwave. It is thought that it may have been reinforced by a teleconnection with ENSO, in particular.

Details of the strength, duration and structure of the 2014–2016 'Blob' can be studied in the ORAS5 charts. The 'Blob' is a unique event in the ORAS5 record and its impact on the marine ecosystem was disastrous. At the time of writing, it was unclear whether the current marine heatwave in the same area will be swept away during the winter storm season or whether it is here to stay.

The ORAS5 page is at: https://www.ecmwf.int/en/forecasts/charts/oras5/.

The ORAS5 NRT page is at: https://www.ecmwf.int/en/forecasts/charts/oras5_nrt/.

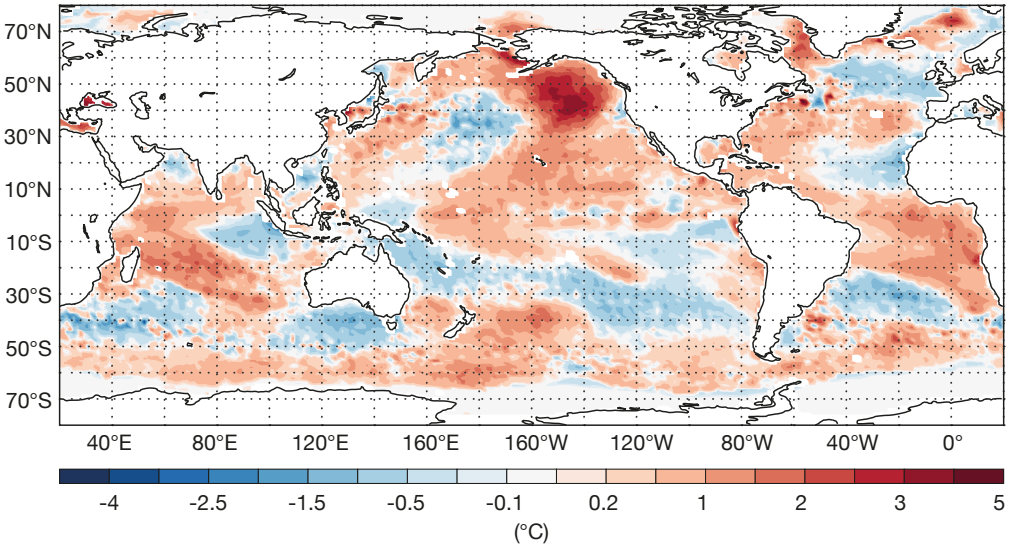

Sea-surface temperature (SST) anomaly on 26 November 2019. This Ocean5 NRT chart shows the SST anomaly on 26 November 2019 computed with respect to the 1993–2016 climate from ORAS5. This kind of chart and many more are freely available to view and download on the ORAS5 and Ocean5 NRT pages on ECMWF's website.

The 1994 Piedmont flood revisited

Enrico Ferrero (University of Eastern Piedmont), Gianpaolo Balsamo (ECMWF)

In the 1994 Piedmont flood in northwest Italy, 77 people lost their lives and the Piedmont region suffered 14.5 bn dollars in economic losses, making this the second costliest European extreme weather event between 1970 and 2012 as documented by the World Meteorological Organization. Twenty-five years on, experts meeting in Italy used modern forecasting systems to reanalyse and re-forecast the rainfall that caused the event.

Forecasts then…

A third of the precipitation falling in one year in Piedmont was observed in 72 hours between 4 and 6 November 1994. The large-scale circulation saw an Atlantic trough extending from the British Isles to the Iberian Peninsula and a blocking high over central Europe. The northward flux from the Mediterranean Sea provided moist air that sustained the precipitation over northern Italy.

At the time, ECMWF predicted the event three to four days in advance. In 1994, the Centre's operational high-resolution forecast used a grid spacing of about 100 km and 31 vertical levels to describe the atmosphere, while an experimental 32-member ensemble forecast had a grid spacing of about 300 km.

…and now

On 6 November 2019, experts in weather forecasting, hydrology and civil protection came together for a workshop in Alessandria, organised by the University of Eastern Piedmont (UPO) and AISAM (Italian Association of Atmospheric Sciences and Meteorology), to analyse the Piedmont flood and the progress made in forecasting extreme events. Thanks to the availability of ECMWF's new ERA5 climate reanalysis, a set of re-forecasts for this major flood was produced using different forecasting systems, including:

- ECMWF's operational Integrated Forecasting System (IFS Cycle 46r1) at grid spacings of 18 km (ensemble forecasts, ENS) and 9 km (high-resolution forecasts, HRES)
- COSMO-2I-EPS (Ensemble Prediction System over Italy) at 2.2 km, with boundary conditions provided by ECMWF ENS.

It was found that all modern-day forecasts made more accurate predictions, and provided better guidance at longer lead times, than ECMWF's forecasts at the time. For example, a 48-hour forecast for 4 and 5 November 1994, produced using the COSMO-2I-EPS system, predicted accumulated rainfall very close to the observed 200 mm in the southern part of Piedmont and close to the 400 mm observed in the western Alpine and pre-Alpine areas.

A comparison of global reanalyses (ERA-Interim and ERA5) and regional reanalyses (such as MERIDA)

Flood impact. The Piedmont flood of 1994 caused dozens of casualties and extensive damage. (*Photo: Associazione Spazioidea - Alessandria*)

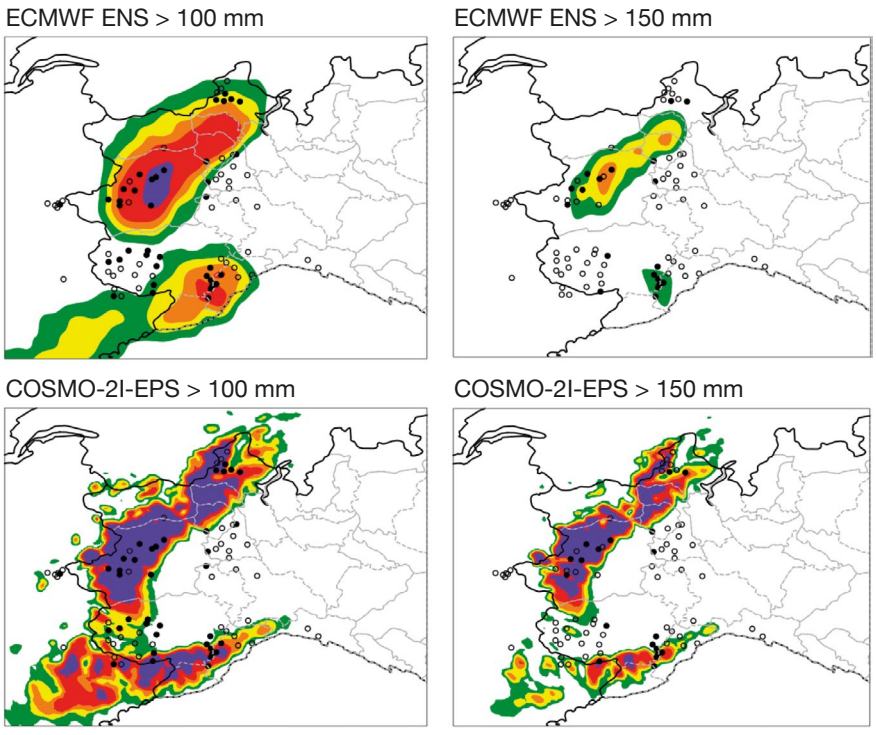

Total precipitation forecasts. The charts show modern re-forecasts, starting at 00 UTC on 3 November 1994, of the probability that total precipitation on 5 November 1994 will exceed the thresholds indicated, for an ECMWF re-forecast at a grid spacing of 18 km resolution (top row), and for a COSMO-2I-EPS re-forecast at a grid spacing of 2.2 km (bottom row). (*Plots courtesy of I. Cerenzia and G. Pincini, Arpae Emilia-Romagna*)

highlighted the value of increased spatial resolution for a detailed reconstruction of events of this kind. A classification of the most extreme precipitation events leading to destructive flooding in northern Italy identified anomalies in integrated water vapour transport from the surface up to 300 hPa and three associated categories of large-scale flow as clear percursors of such events.

Conclusion

In the final discussion, it was concluded that today's modelling capabilities make it possible to predict cases such as the 1994 Piedmont flood with satisfactory accuracy. Similar events that occurred on 21 October and 23–24 November 2019 caused flooding, but the impact on the population was much reduced thanks to progress in forecasting and in the alert chain involving national civil protection and regional environmental protection agencies. However, especially in the context of global warming, the fact that such events can be extremely localised and can develop over a very short period of time represents new challenges for numerical weather prediction.

A special issue of the *Bulletin of Atmospheric Science and Technology* will collect scientific contributions from the workshop until September 2020.

Recent BUFR dropsonde data improved forecasts

Bruce Ingleby, Fernando Prates, Lars Isaksen, Massimo Bonavita

On 4 September 2019, ECMWF started operationally assimilating dropsonde reports in the BUFR format. By coincidence this was during the active phase of Hurricane Dorian. Since this was a storm of considerable interest and also well observed by dropsondes, the period was rerun with a) no dropsonde data ('NoDrop'), b) only alphanumeric dropsonde data ('ADrop'), c) BUFR dropsonde data instead of the alphanumeric reports where both are available ('BDrop'). The results, shown in the figure, cover four tropical cyclones (including Dorian) and six tropical storms. They suggest that BDrop is slightly better than the other experiments, especially for intensity. On average, the central pressure was overestimated, but by less in the BDrop experiment. The sample size is rather small, but because of the intermittent nature of dropsonde availability, sample size is usually an issue. Earlier experiments looking at a six-week period in September/October 2018 showed a neutral impact of the BUFR dropsonde data (BDrop vs ADrop, not shown).

Advantages of using BUFR data

The 2018 experiments were also used to test the assimilation of low level height data from the dropsonde reports (almost equivalent to assimilating pressure at mean sea level). This is included in the BDrop results shown and in the operational implementation. Alphanumeric dropsonde reports often only have 10 to 30 levels. Some of the BUFR reports, on the other hand, have high vertical resolution (typically about 200 to 900 levels, depending partly on the height of the drop). Some thinning is applied before the assimilation, so that 25 to 30% of these levels are assimilated. Overall, almost six times as many dropsonde wind levels were assimilated in the BDrop experiment as in the ADrop experiment. The BUFR reports also contain the horizontal position of the dropsonde at each level. This makes it possible to account for downwind drift. For the trial periods, the dropsonde drift was relatively modest (20 to 30 km at most).

Slow migration

While increasing numbers of high-resolution BUFR radiosonde ascents have been assimilated at ECMWF since late 2014, the migration of dropsonde data to BUFR has been relatively slow by comparison. In autumn 2018, real-time high-resolution BUFR dropsonde reports became available from some NOAA (US National Oceanic and Atmospheric Administration) flights. In the 2019 hurricane season, high-resolution BUFR reports also became available from some US Air Force flights and from one flight by the Hong Kong authorities (the profiles from the US flights were also available as alphanumeric reports, but the Hong Kong data were BUFR only). Many tropical cyclones are not sampled by dropsondes at all, and in those cases forecast skill is heavily dependent on the good use of satellite data.

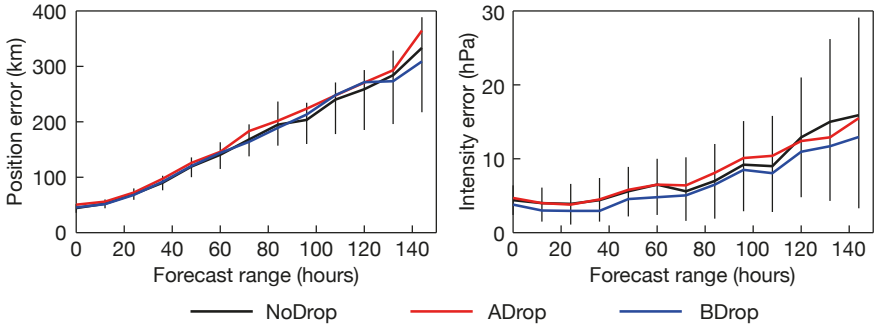

Position and intensity errors in tropical cyclone forecasts. The left-hand panel shows the average position error and the right-hand panel the average intensity error in ECMWF high-resolution (HRES) forecasts compared to tropical cyclone advisories, for forecast starting dates from 26 August to 8 September 2019 and two forecasts per day. For NoDrop, the 5% and 95% percentiles of the distribution, estimated using a bootstrap procedure, are given. For the other experiments, the percentile bars are similar and tend to move up and down with the mean. The sample size is about 100 at analysis time and 22 after six days (the numbers decline because the storms dissipate both in reality and in the experiments).

Progress towards assimilating visible radiances

Angela Benedetti, Samuel Quesada-Ruiz, Julie Letertre-Danczak, Marco Matricardi (all ECMWF), Gareth Thomas (RAL Space)

Satellite observations in the infrared and microwave parts of the spectrum have long been assimilated into forecasting systems to help estimate the best possible initial conditions for global weather predictions. Assimilating radiances in the visible part of the spectrum, on the other hand, continues to pose many challenges. The reason lies in the complex respective interactions of cloud and aerosol particles with radiation at those wavelengths as well as the complex characteristics of the surface as a reflector of visible light. These complications make it difficult to develop 'observation operators', which convert model values into satellite observation equivalents. However, progress towards assimilating visible radiances has recently been made in the context of the ARAS (Aerosol Radiance Assimilation Study) project funded by the European Space Agency (ESA).

Assimilating aerosol data

As part of ARAS, an observation operator based on the Oxford-RAL Aerosol and Cloud (ORAC) satellite retrieval scheme has been developed and incorporated into ECMWF's Integrated Forecasting System (IFS) with the help of the RAL (Retrieval of Aerosol and Cloud) group. This operator includes look-up tables in which reflectances at the top of the atmosphere are stored as a function of aerosol optical properties such as optical depth, single scattering albedo and asymmetry parameter as well as satellite viewing geometry and the position of the sun. Optical depth is associated with the amount of radiation scattered or absorbed by aerosols, while the single scattering albedo essentially gives an indication of the part that is absorbed and the asymmetry parameter of the part that is scattered. Observations used in the ARAS project are the level 2 aerosol visible radiances (reflectances) from the MODIS instrument on board the Aqua and Terra satellites. This is the first time that this type of observation has been assimilated in ECMWF's atmospheric 4D-Var assimilation system. While assimilating such observations is still experimental, the results show great potential for future operational implementation in the atmospheric composition forecasts produced by the EU-funded Copernicus Atmosphere Monitoring Service (CAMS) implemented by ECMWF.

A dust event coming from the Sahara desert on 1 March 2017 illustrates what difference the assimilation of visible radiances can make. The figure shows total aerosol optical depth (AOD) at 550 nm in the IFS analysis without any assimilated aerosol data and with the assimilation of MODIS visible reflectances, as well as satellite-derived AODs from MODIS at the same wavelength. In this event, MODIS observed two plumes. The first one, crossing the Atlantic Ocean at around 10°N, is underestimated in the analysis. The assimilation of radiances increases AOD in the analysis to a level comparable to the MODIS data. The second plume in the Gulf of Guinea is mostly missed in the analysis without any assimilated aerosol data. The assimilation of the radiances brings clear benefits in this case.

Outlook

ARAS is scheduled to finish in April 2020, but its outcomes will hopefully be useful to other applications. For example the new release of the RTTOV observation operator includes an extension to calculate radiances in the visible part of the spectrum for cloudy conditions based on the look-up table approach. From a formal point of view, treating clouds or aerosols via this approach is very similar. This implies that many of the tools developed in ARAS for aerosol visible reflectance assimilation could be adapted for clouds, provided the appropriate look-up tables are used. The use of visible radiances for cloud assimilation would be a major step forward as these data are currently not assimilated at all at any operational numerical weather prediction centre, even though they provide crucial information on the state of the atmosphere in cloudy conditions. More research is still needed, but the results from the aerosol assimilation achieved in ARAS could open the way towards a fuller exploitation of visible radiances to improve numerical weather prediction.

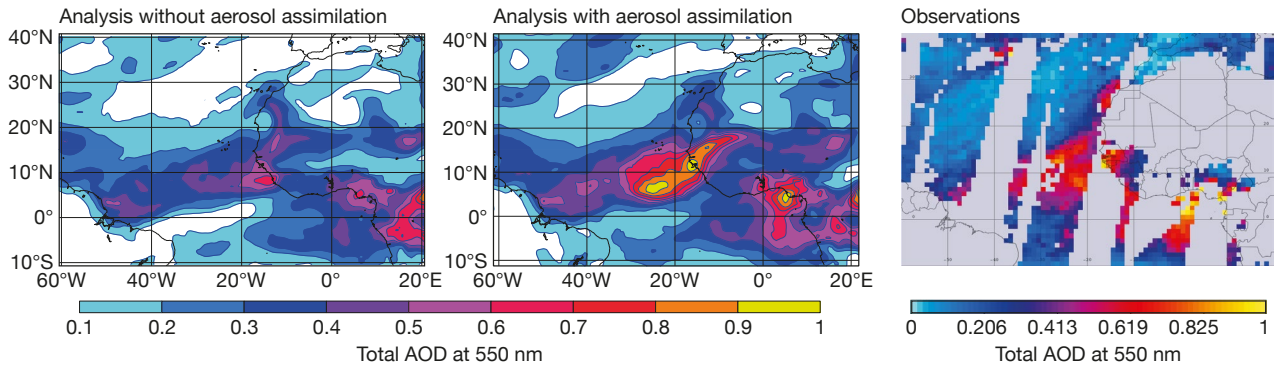

Impact of assimilating aerosol data. The left-hand plot shows total aerosol optical depth (AOD) at 550 nm in ECMWF's analysis for 12 UTC on 1 March 2017 without the assimilation of aerosol information; the middle plot shows the same with the assimilation of MODIS reflectances at two different wavelengths (670 nm and 866 nm); and the right-hand plot shows total AOD at 550 nm from MODIS on Terra for 1 March 2017.

A heat health hazard index based on ECMWF data

Claudia Di Napoli, Christopher Barnard, Christel Prudhomme, Florian Pappenberger

ECMWF has begun to produce pre-operational forecasts of a heat health hazard index in real time using meteorological forcing data from its Integrated Forecasting System (IFS). The high-resolution and probabilistic forecasts, which predict the Universal Thermal Climate Index (UTCI) at the global scale, will become available to users in the second half of 2020.

The production of human thermal stress data from ECMWF's meteorological products answers the call, issued by the World Meteorological Organization in 2004, to incorporate biometeorological forecasts into the suite of products and services offered by meteorological and hydrological services. Biometeorological forecasts consist in the prediction of weather-related conditions, such as thermal stress due to extremes of heat and cold, that might negatively impact human health. Extreme heat, for instance, is responsible for a variety of risks, including dehydration, cramps, and even death, especially during sustained periods of high temperatures (heatwaves). Mortality and other health problems (frostbite, hypothermia) can also occur as a result of exposure to extreme cold.

Calculating the index

The UTCI is a state-of-the-art indicator representing the thermal (heat and cold) stress of the human body. It is calculated using an advanced model of human thermoregulation coupled with a clothing insulation model.
The models estimate the effect of air temperature, wind speed, water vapour pressure and short- and long-wave radiant fluxes on human physiology. The UTCI takes values on a stress category scale ranging from extreme cold stress to extreme heat stress. A pre-operational system has been developed at ECMWF to produce UTCI forecasts in real time. The system uses as forcings the forecasts of air temperature, humidity, wind speed and mean radiant temperature (MRT) from ECMWF's Integrated Forecasting System (IFS). MRT is a critical physical quantity representing how human beings experience radiant fluxes. Its automatic computation is fully integrated into the system. UTCI and MRT outputs are generated at the same time as ECMWF's extended-range forecasts up to 46 days ahead.

Reanalysis data

The system has also been used to generate historical datasets of UTCI and MRT based on the ERA5 reanalysis. The datasets currently span the period from 1979 to the present and provide a record of thermal stress in past extreme events. Reanalysis UTCI gridded data for the June 2019 European heatwave, for instance, show widespread conditions of thermal stress across the continent. As can be seen in the figure, extreme heat stress hazardous to human health occurred in parts of Spain, France and Italy.

Reanalysis UTCI and MRT data are now available for download through the Climate Data Store run by the Copernicus Climate Change Service (C3S) implemented by ECMWF. Forecasts and reanalysis data will be archived in ECMWF's Meteorological Archival and Retrieval System (MARS) from the second half of 2020.

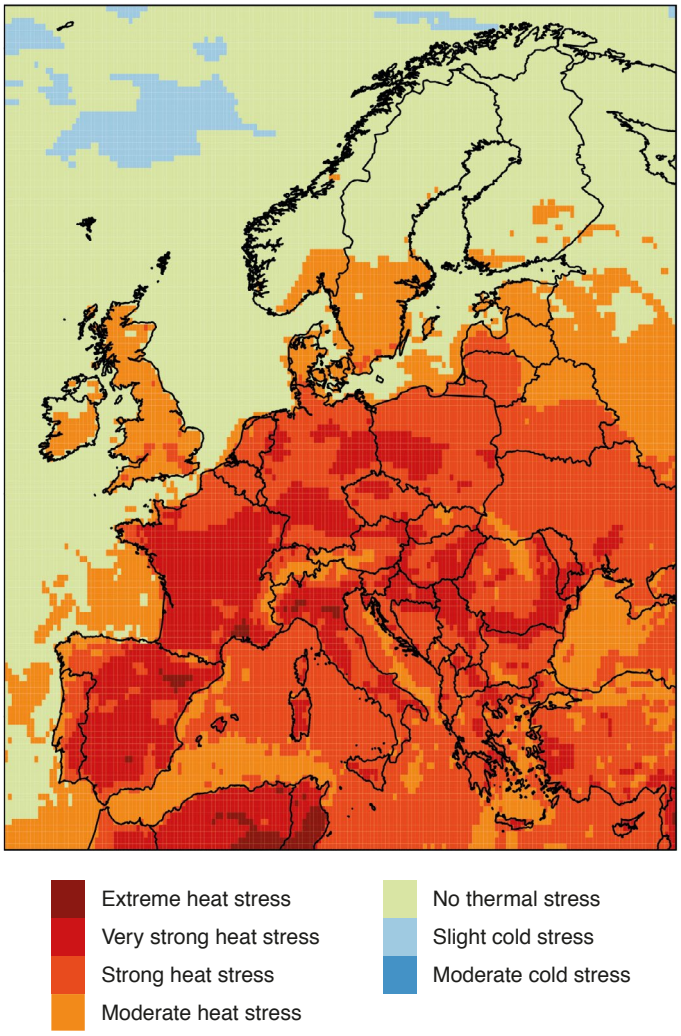

Heat stress during the June 2019 heatwave. The map shows locations where conditions of heat stress, as represented by UTCI reanalysis data, occurred between 24 June and 2 July 2019 in Europe.

ECMWF's new IT network and security infrastructure in Bologna

Ahmed Benallegue

The planned move of ECMWF's computing capabilities to a new data centre in Bologna, Italy, presents a unique greenfield deployment opportunity: the installation and configuration of a network where none existed before. This happens very rarely in the lifetime of an organisation. It was therefore vital to design a network and security infrastructure that is both innovative and future-proof whilst ensuring the best possible performance for the benefit of ECMWF's Member and Co-operating States and end users. This article describes briefly the new design and outlines the steps that will be taken to ensure a smooth migration from Reading to Bologna.

Key requirements

ECMWF's current Network and Security (N&S) architecture in Reading is centred on a multi-layer core with perimeter security design. It is widely acknowledged that this type of architecture can no longer fulfil the requirements of modern data centres. Therefore, it was decided to introduce a new architecture in Bologna which can quickly adapt to ever-changing configurations, based on the following requirements:

- **Virtualisation and cloud-native technologies**: ECMWF already provides services running in private and public clouds. It is therefore crucial to have an infrastructure that enables the use of and protects all services wherever they are hosted.
- **Scalability, reliability and performance**: it is essential to ensure that the network provides reliable connectivity with the highest possible bandwidth whilst being able to expand easily and quickly when required.
- **'Defence in depth'**: the security challenges raised by modern IT environments require a different cybersecurity approach, in which defensive mechanisms are layered in order to protect valuable data and information.
- **Automation and orchestration**: the introduction of management tools will simplify the configuration and monitoring of the N&S infrastructure, giving the capability to operate and configure the infrastructure remotely and enable faster deployment and operation of modern dynamic applications.

The new design

The following are the main architectural elements of the new N&S design:

- **'IP Fabric' architecture**: this is a state-of-the-art network architecture for medium- and large-scale data centres comprising two layers: leaf switches, to which systems connect, and spine switches, to which leaf switches connect. This architecture minimises delays and bottlenecks whilst offering greater scalability, reliability and performance.
- **Multi-site topology**: two physically

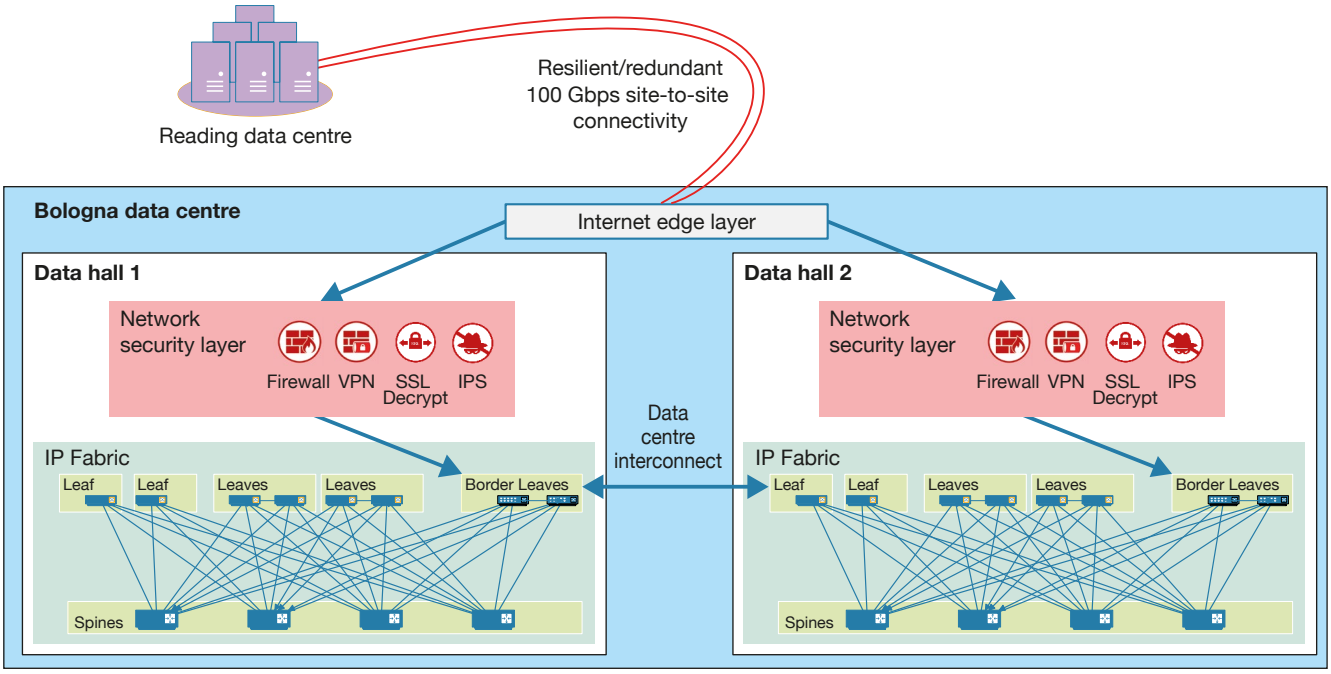

High-level overview of the new network and security design. An IP Fabric network and its associated network security infrastructure is deployed in each data hall. The two networks will be interconnected through a data centre interconnect link. To cater for the anticipated data transfer from Reading to Bologna, 100 Gbps site-to-site fully redundant connectivity will be put in place temporarily.

segregated IP Fabric networks will be deployed in the new data centre: one in each data hall, thus creating two separate fault domains. This will significantly increase the availability of the resulting services as outages and maintenance sessions will impact only one hall at a time.

- **Security layer**: the segmentation of the data centre network into different security zones will offer higher control and visibility of data traffic. In addition, new security defence controls will be introduced to improve the operational security and therefore the ability to prevent and react to internal and external threats.

Progress to date

Following the formal design validation by ECMWF's Technical Design Authority in October 2018, the various components of the N&S infrastructure have been procured through multiple invitations to tender. A pilot infrastructure, compromising the main components of the N&S infrastructure, was built at the Reading site and was subjected to a comprehensive set of tests. This resulted in the formal acceptance of the IP Fabric infrastructure on 29 November 2019.

What will happen next?

The N&S pilot infrastructure will be moved to the new data centre in Bologna as soon as the site is ready. In the meantime, work has already started with service and application owners to ensure a smooth transition from Reading to Bologna.
The suitable N&S design for each service or application will be defined and subjected to validation tests using the pilot infrastructure. If you are interested in learning more, please feel free to contact Ahmed Benallegue, Leader of the Networks and Security Team (ahmed.benallegue@ecmwf.int).

Computing Representative meetings to become more interactive

Anna Ghelli

This year's meeting of ECMWF Computing Representatives took place from 23 to 25 October 2019 and was attended by 27 participants. The event included new interactive sessions and this aspect is expected to be strengthened further in future meetings.

Computing Representatives are appointed by ECMWF Member and Co-operating States and meet regularly at the Centre to share experiences on computing services. They are points of contact for ECMWF and facilitate the information flow and various administrative transactions between the Centre and countries that have access to ECMWF's computing services.

The programme of this year's meeting included updates on ECMWF's BOND (Bologna Our Next Data Centre) project, new services, and innovation projects, such as the European Weather Cloud. The participants appreciated two new interactive sessions: a live demonstration event to present the new services, and a 'Meet the expert' session where participants could ask questions and have face-to-face discussions with ECMWF experts. The participants gave short overviews of activities in their own countries, showcasing their new computing services, high-performance computing procurement processes and use of ECMWF's computing facilities. This sharing session was valued as it allowed participants to discover each other's activities and develop collaborations.

Finally, the participants offered feedback on the meeting itself and potential ways to improve the format. It was generally felt that the length of the meeting is appropriate, but participants would like to have longer interactive and 'active' sessions. Future meetings could feel more like a forum to encourage sharing and networking among participants and ECMWF experts. We look forward to welcoming our Computing Representatives next year.

Presentations from this year's meeting are available at: https://www.ecmwf.int/en/about/who-we-are/representatives/computing-representatives.

Group photo. Twenty-seven Computing Representatives and several ECMWF members of staff attended the meeting at ECMWF's headquarters in Reading, UK.

Data archive growth: Escaping from the black hole

Paul Burton, Bentorey Hernandez Cruz

Continuing to increase the size of ECMWF's data archive at historical rates is becoming unsustainable due to rising costs. To limit future growth, the Centre has developed a tool to facilitate the removal of obsolete data, and it will take measures to reduce the amount of data written into the archive.

Archive growth

The data archive, comprising the MARS (Meteorological Archival and Retrieval System) database for structured meteorological data, and ECFS (ECMWF File Storage) for all other data, has been an indispensable part of the computational infrastructure of ECMWF for many years. It allows researchers to easily examine, share and compare results from their experiments, supporting the continual improvement of the Integrated Forecasting System, whilst also providing an invaluable long-term archive of operational forecast and reanalysis data for use both inside and outside ECMWF.

Due to the good design and implementation of the data archive system, there has been an almost irresistible temptation to treat it as a black hole for data, with users simply adding ever increasing amounts into the archive every year. The graph shows the amount of data users have written into the archive over the past seven years. The growth of the archive is exponential, increasing at a rate of around 45% per year – driven by the ever-increasing computational power of ECMWF's high-performance computing (HPC) resources. Historically we accommodated the archive growth by simply buying more tapes and associated hardware. This technology grew cheaper at a rate corresponding to the increase in HPC performance per dollar, meaning the relative financial cost of the archive to the HPC resource stayed stable. However, over recent years the cost of archive storage has almost stagnated, therefore increasing the size of the archive at historical rates is becoming unsustainable within existing budgets.

New tool

To address this unaffordable growth, two big purges have taken place in the research data archive over the last four years, which together have removed over 100 PiB of data. The total archive, however, is still growing at an unsustainable rate, so further action is now being taken.

We have developed a Data Lifetime Management (DLM) Tool which allows research users to classify all their experimental data according to its expected use (e.g. 'test'/'long-term reference'/'publication'). Each classification has a lifetime associated with it, and when a given dataset has exceeded its lifetime, its owner is prompted to either delete it or reclassify it. The tool is under active development to give users more information about their data and how it is being used, which will allow them to manage its lifetime effectively.

Deleting old data is only a temporary solution, however; the fundamental issue is to reduce the amount of data being written into the archive. To this end, an Archive Working Group has been convened which will be considering how this can be achieved, addressing all users of the ECMWF archive, including research users, Copernicus and reanalysis activities, and our operational forecasting system.

The changes in behaviour that will happen as a result of the DLM and Archive Working Group will mean an end to treating the data archive as a black hole for data; there will be some difficult decisions to be made on our journey to reducing the amount of data written to the archive – but the reward will be an affordable and sustainable data archive that can continue to support the activities of ECMWF and its Member States for many years to come.

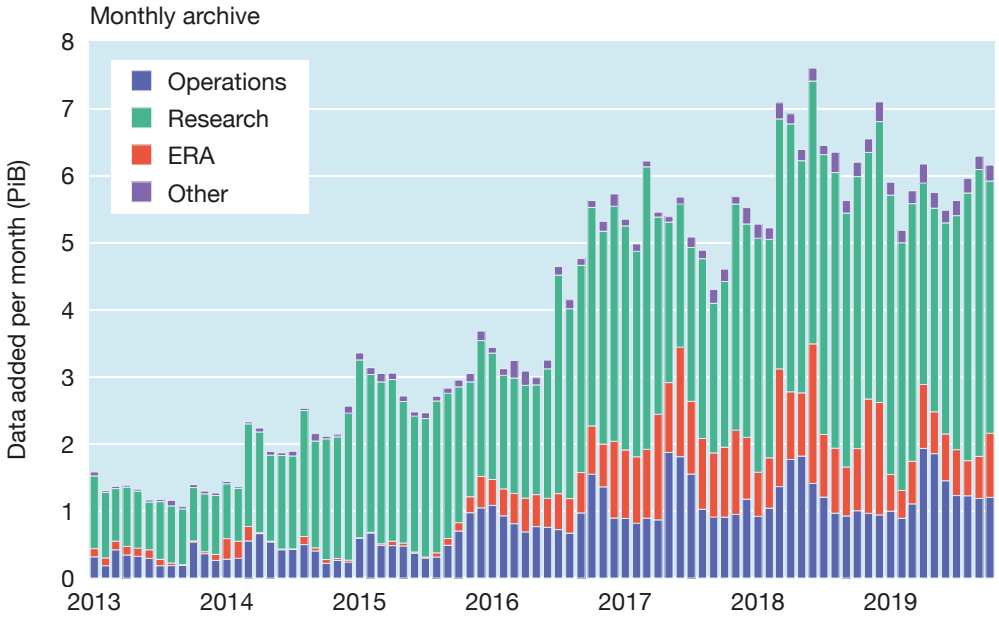

Data archive growth. The increase in the growth of ECMWF's data archive has been driven by three areas: research, the ERA-Interim and ERA5 weather and climate reanalyses, and operations.

GAIA 5.0: A science–art project using ECMWF data

Renate C.-Z.-Quehenberger (philosopher and independent art researcher),
Louise Arnal, Kristian Mogensen (both ECMWF)

Over the last year, artist and philosopher Renate C.-Z.-Quehenberger collaborated with scientists at ECMWF (Louise Arnal and Kristian Mogensen) and at the European Commission's Joint Research Centre (Rita Van Dingenen, Thomas Petroliagkis and Frank Raes) on her science–art (SciArt) project GAIA 5.0: A Holographic Image - Ambience. This was created for the JRC's Resonances III festival and exhibition from 15 October to 8 November 2019 in Ispra, Italy. The work was also shown at the BOZAR Centre for Fine Arts in Brussels from 5 December 2019 to 19 January 2020.

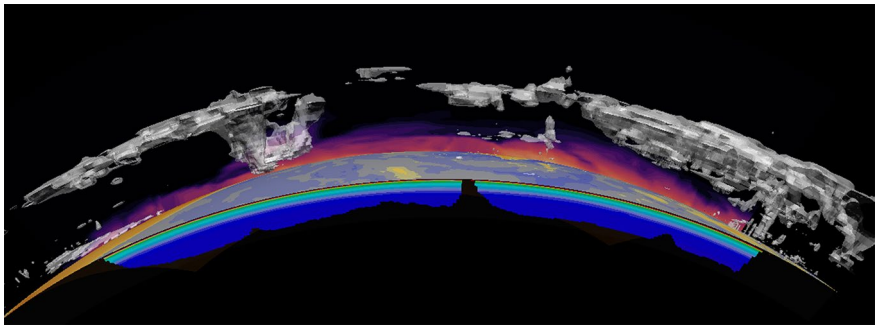

Still from the 3D animated visualisation and VR experience GAIA 5.0. The image shows a 3D representation of the tropical cyclones Luban and Titli above the Indian Ocean, reconstructed using ECMWF data on ocean temperature, humidity and clouds. The red and purple shading shows humidity, while the pale blue and yellow areas show sea-surface temperature and the cross section of the ocean shows temperature. (*Image: Leyla Kern/HLRS*)

The centrepiece of the project is a 3D animated video art work based on ECMWF data for two tropical cyclones, Luban and Titli, which developed in early October 2018 over the Arabian Sea and the Bay of Bengal, respectively. It was presented as a hologram installation and as an interactive Virtual Reality (VR) experience.

During a visit to ECMWF in May 2019, Louise Arnal and Kristian Mogensen provided Renate Quehenberger with ECMWF data for the two tropical cyclones. The data were ERA5 reanalysis data together with ocean data from a simulation produced using the community ocean model NEMO with ERA5 forcing data. The variables provided included geopotential height, surface pressure, ocean depth, wind components, cloud coverage, humidity and temperature. Visualisations of the data were created at the High Performance Computing Center (HLRS) in Stuttgart, Germany, using the visualisation software COVISE and VISTLE together with the OpenCover renderer. The software enables interactive exploration of immersive environments and supports the processing of large datasets. It was adapted to the needs of the project, for example by enabling it to read netCDF files. The data were processed at HLRS by Leyla Kern and the head of visualisation, Uwe Wössner. The result was a visual reconstruction of the meteorological event as a combination of oceanic and atmospheric dynamics.

The visualisation of coupled atmosphere–ocean dynamics, including the way in which tropical cyclones are fuelled by heat from the ocean, can help viewers to gain a better understanding of the complexity of the Earth system and extreme event generation. By being aesthetically pleasing, the animation attracts an audience with no prior knowledge of the subject matter and communicates the science in a more approachable way than other modes of presentation.

For more information, visit: https://resonances.jrc.ec.europa.eu/installation/gaia-50-holographic-image-ambience.

New observations since October 2019

The following new observations have been activated in the operational ECMWF assimilation system since October 2019:

Observations	Main impact	Activation date
Scatterometer winds from ASCAT on Metop-C	Near-surface winds over ocean	2 December 2019
Radiances from MWHS-2 on FY-3D	Humidity, clouds, dynamics	2 December 2019
Soil moisture from ASCAT on Metop-C	Soil moisture, screen-level parameters	10 December 2019
Atmospheric Motion Vectors from GOES-17 (replacing GOES-15)	Tropospheric wind	10 December 2019

EFAS upgrade improves performance and updates forecast products

Corentin Carton de Wiart, Louise Arnal, Maurizio Latini, Blazej Krzeminski, Tiago Quintino, Christel Prudhomme

The European Flood Awareness System (EFAS) has been operational as part of the Copernicus Emergency Management Service (CEMS) since 2012. ECMWF's role in EFAS includes running the hydrometeorological computations, archiving the data and disseminating the forecasts. While EFAS development over the years has focused mainly on new products, an upgrade to EFAS v3.3 implemented on 8 October 2019 aimed to improve the operational workflow and the presentation of existing products.

ECMWF has worked with the European Commission's Joint Research Centre (JRC), which runs CEMS, and the EFAS consortium to redesign the workflow to prepare for future resolution increases and new products. This was an opportunity to improve performance and upgrade the medium-range forecast products, following feedback from EFAS partners.

Medium-range forecast product upgrade

On the design side, a new forecast layer now provides an overview of 'reporting points'. These are dynamic points, generated each time a new forecast is produced, in locations where an elevated flood risk is expected in the next 10 days. The reporting points are shown together with locations for which no flood risk is predicted but where hydrological information is shared by EFAS partners (the 'static points'). This new design gives users a complete and coherent overview, in a single layer, of all locations at which EFAS medium-range forecasts are accessible. It also enables partners who have shared their hydrological data with the EFAS consortium to monitor the hydrological evolution of their catchments of interest. This was not possible before if the predicted flood signal did not reach an EFAS-defined threshold. In addition, the way the reporting points are displayed has also been improved. As shown in the figure, stations with an elevated flood risk are quickly identifiable (red and yellow squares), facilitating the work of the forecasters on duty at the EFAS dissemination centres (the hydrometeorological services of Sweden, the Netherlands and Slovakia).

Performance gains

The expected growth in the number of EFAS partners, and thus of reporting points, together with the envisaged increase in resolution of EFAS products motivated a full review of the existing product generation chain to enable greater scalability and prepare for future upgrades. This was also an opportunity to reduce the complexity of the legacy tools that make up the operational suite, which used a mix of programming languages, such as Python, R, PCRaster, C++ and bash scripts. The new product generation is based on a newly developed Python framework called 'danu'. This framework aims to:

- gather common functionalities of flood forecasting in a shared framework
- improve modularity of the system, allowing easier implementation of new features
- improve maintainability using modern software engineering processes
- promote collaborative development practices between hydrologists and computer scientists
- introduce parallel computing and data hypercubes into the process, preparing the system for the next resolution upgrade.

Using parallelism in compute-intensive parts of the workflow has led to dramatic performance gains, from 5 times faster for alert generation to up to 50 times faster for ensemble statistics. Porting the multiple processes into a single framework also made it possible to optimise filesystem I/O by avoiding data transfers, which was a major performance bottleneck. These performance improvements were achieved thanks to close collaboration between the scientists that developed the system and computer scientists that reworked it, creating positive feedback where technical developments empower the science to go further. The tools developed in the Python framework 'danu' and this successful collaboration between teams are now being applied to other environmental forecast modelling chains, such as those developed for the EU-funded SMUFF project 'Seamless probabilistic multi-source forecasting of heavy rainfall hazards for European flood awareness'.

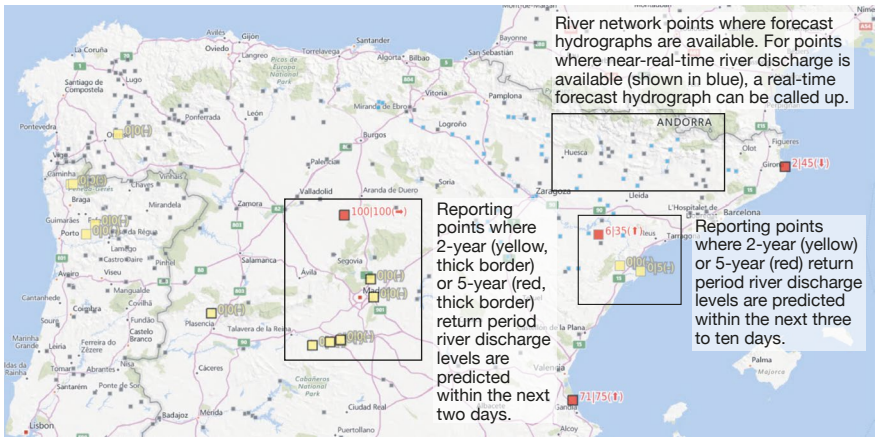

New layer for reporting points and static points. A new layer shows all river network points where forecast outputs are available (reporting points and static points) in a single view.

ECMWF supports the South-East European Multi-Hazard Early Warning Advisory System

Fredrik Wetterhall, Umberto Modigliani (both ECMWF), Milan Dacić, Sari Lappi (both WMO)

In January 2020, ECMWF became involved in the second phase of the project to build a 'South-East European Multi-Hazard Early Warning Advisory System' (SEE-MHEWS-A), which aims to strengthen the existing early warning capacity in the region. The project was initiated in 2014 by the World Meteorological Organization (WMO) and the US Agency for International Development (USAID). It is currently funded by the World Bank, through the Global Facility for Disaster Reduction and Recovery, and by the European Union. For 18 months, the project will test a prototype of a flood early warning system using local information and multiple models to better characterise the flood risk in selected catchments.

ECMWF's role in the project

ECMWF's role in the project will be to support the implementation of the system, the tuning of the models, and the dissemination of the results through a web interface. The three areas in which ECMWF will be involved are:

- supporting the installation and customisation of a pilot version of the Centralised Observational Database (CODB) based on ECMWF's data acquisition and pre-processing system (SAPP) and ECMWF's Meteorological Archival and Retrieval System (MARS) to support the envisaged suite of coupled meteorological, hydrological and marine/oceanographic models
- supporting the implementation in an operational environment; the calibration and verification of the hydro-meteorological modelling chain, building on tools that ECMWF is already operating for the Copernicus Emergency Management Service (CEMS); and further post-processing of hydrological outputs
- supporting the setting up of limited-area model runs in the ECMWF environment and thus supporting the demonstration of cascading forecasts with multiple numerical weather prediction models at global, regional and local scales.

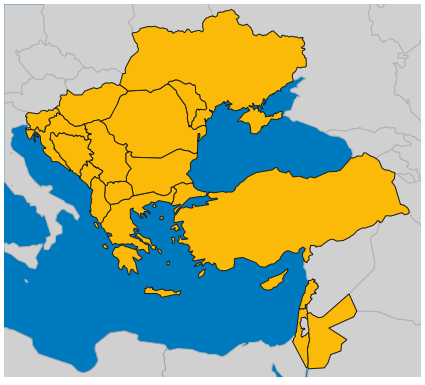

Countries covered by SEE-MHEWS-A. Albania, Bosnia and Herzegovina, Bulgaria, Croatia, Cyprus, Greece, Hungary, Israel, Jordan, Lebanon, Montenegro, Republic of Moldova, Romania, Serbia, Slovenia, North Macedonia, Turkey, Ukraine.

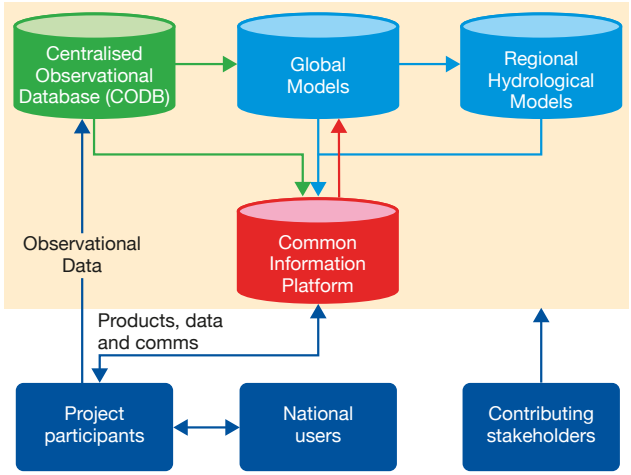

SEE-MHEWS-A setup. The diagram shows the suite of coupled meteorological, hydrological and marine/oceanographic prediction models in SEE-MHEWS-A as well as their links with a centralised observational database using SAPP technology and with a common information and communication platform.

The work will be carried out by expert teams contracted by the World Bank and the WMO for the project. The role of ECMWF is to support these experts in their work in relation to ECMWF's high-performance computing facility and its IT/software frameworks (SAPP, ecFlow, and similar packages).

Technical setup

The project needs temporal and spatial observations of high resolution across the region. These data already exist but are not exchanged as this goes beyond the minimum required by WMO data exchange policies. Observations will be converted to BUFR using SAPP. These data will then be used in the data assimilation for the initial conditions of the meteorological and hydrological chain, and for tuning and calibration of the hydrological model.

The implementation of state-of-the-art transboundary hydrological forecasting systems in an operational setup requires complex expertise, software and tools. This can be beyond the reach of national hydrological services. Through CEMS, ECMWF has gained solid expertise in setting up, running and verifying coupled hydrometeorological forecasting systems. SEE-MHEWS-A will provide an opportunity for ECMWF to transfer this expertise to Member and Co-operating States in the region by supporting the implementation of such a complex state-of-the-art system.

Further information

More details about the SEE-MHEWS-A project are available on the WMO project web page: https://public.wmo.int/en/projects/see-mhews-a.

Users continue to rate Copernicus services highly

Kevin Marsh, Anabelle Guillory, Michela Giusti, Xiaobo Yang

The 2019 user satisfaction surveys for the two EU-funded Copernicus services implemented by ECMWF show that the vast majority of users remain highly satisfied. Survey results for the Copernicus Climate Change Service (C3S) and the Copernicus Atmosphere Monitoring Service (CAMS) reflect the growing uptake of the services by the private sector, including within the EU. Participants also made a number of suggestions for improvements.

C3S

The 2,114 users who participated in the C3S survey gave the service an overall satisfaction rating of 4.2 out of 5 stars. Around two thirds of survey participants were based outside the EU, and around 70% were academics and researchers. A comparison of usage patterns and satisfaction ratings from 2017 to 2019 shows that uptake in the private and public sectors continues to grow. Within the EU, there is increasing private sector interest in C3S products, especially in climate reanalysis data.

Climate reanalysis data (mainly ERA5 datasets) continue to be by far the most popular with users across the board and received the highest satisfaction ratings. However, other C3S products and services, such as seasonal forecast datasets, have increased in popularity. Users also found the Copernicus User Support team (CUS), the data access mechanisms (such as the Climate Data Store API), and the extensive documentation useful.

C3S user feedback

The following is a sample of some of the user comments from the C3S user satisfaction survey.

"It is a tremendous international asset. Thank you and keep up the good work."

"Excellent platform. Congratulations."

"Many aspects are excellent and world-class. Others are not efficient or unworkable, and need better solutions or support to make data available in practical ways."

"The system is very nice but needs improvements."

"The quality of data themselves is state-of-the-art."

"The API is a great tool and makes my life much easier."

"Forum is very helpful."

As in previous years, the survey participants made many suggestions for improvements, particularly in relation to data retrieval from the Climate Data Store and the Toolbox. The survey results indicated that the C3S newsletter and the new CUS Forum should be used to strengthen communication with users and to help build a C3S user community. This is in line with the CUS vision of developing 'self-service' user support capabilities.

CAMS

The 120 users who participated in the CAMS survey gave the service a satisfaction rating of 4.3 out of 5 stars. Around 62% of participants were based in the European Union, and around 45% of them worked in academia/research, while 25% were based in the business sector – a higher figure than for C3S. As with C3S, interest in CAMS from the commercial sector has been increasing over the past three years, particularly within the EU.

The most popular CAMS services were information on global atmospheric composition and global reanalysis. Data access mechanisms, validation reports and product documentation were also seen as very valuable. Areas for improvement identified by users include raising user awareness of air quality products that can provide policy support for decision-makers, such as assessment reports and local pollution forecasts.

Further information

Full 2019 C3S and CAMS user satisfaction survey reports will be available in February 2020 from https://climate.copernicus.eu/help-and-support and https://atmosphere.copernicus.eu/user-support, respectively.

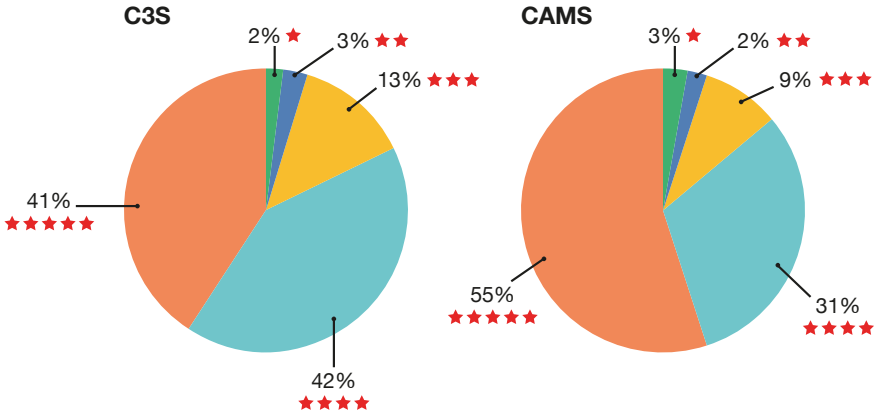

C3S and CAMS overall satisfaction ratings 2019. Respondents to the C3S and CAMS user satisfaction surveys rated the services highly, with 83% awarding C3S four or five stars and 86% awarding CAMS four or five stars.

ERA5 reanalysis data available in Earth Engine

Julia Wagemann

Nine variables in the Copernicus ERA5 global weather and climate reanalysis dataset are now part of the Google Earth Engine's public data catalogue. Earth Engine is a cloud-based data analysis platform widely used by Earth observation practitioners, scientists and researchers. Making a selection of ERA5 data available in Earth Engine makes this powerful reanalysis dataset more easily accessible to the Earth observation community.

Data selection

The EU-funded Copernicus Climate Change Service (C3S) implemented by ECMWF makes petabytes of climate data openly available. The most popular C3S dataset is ERA5, which provides a record of the global weather and climate since 1979 using over 200 variables at a grid spacing of 31 km and at hourly intervals. ERA5 variables are of interest not only to meteorologists and climatologists, but also for land monitoring applications, flood forecasting and climate change impact assessments at country level. Air temperature, wind information and precipitation are some of the variables that are often of interest to environmental monitoring applications and assessments. Although all ERA5 data are freely available via the C3S Climate Data Store, the dataset has not been fully exploited by the Earth observation community as until recently it was not part of Earth Engine's public data catalogue.

The following nine variables have been made available in Earth Engine: minimum, mean and maximum 2-metre air temperature, total precipitation, 2-metre dewpoint temperature, surface pressure, mean sea-level pressure and 10-metre u- and v-components of wind. Three Earth Engine image collections with different temporal aggregations (hourly, daily and monthly) have been made available, enabling efficient data retrievals for different applications. The selection of variables is based on the results of a survey among the Earth Engine community. The hourly ERA5 reanalysis data for all nine variables have a total volume of around 7 terabytes.

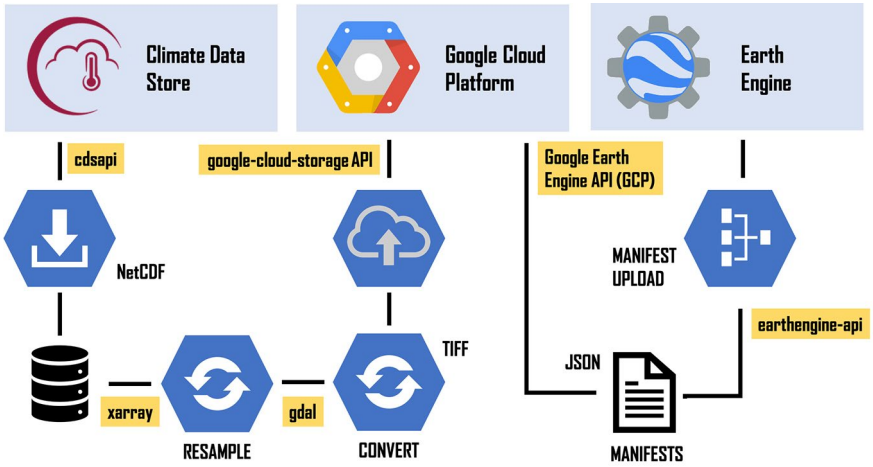

Workflow diagram. ERA5 data from the Climate Data Store are processed in a multi-step workflow before they are made available as assets in the Google Earth Engine.

Interoperability of data systems

The workflow consists of six major steps:

1. Downloading hourly data as daily files or monthly aggregates in NetCDF format from the Climate Data Store
2. Aggregating hourly files to daily means or sums (total precipitation)
3. Converting NetCDF data to GeoTiff
4. Uploading hourly, daily and monthly GeoTiff files to the Google Cloud Platform (GCP)
5. Creating image manifests (JSON-based files) describing the metadata and band name of the resulting Earth Engine asset
6. Ingesting data files uploaded to GCP as assets into Earth Engine with the help of the manifest files.

The project to make the data available took around nine months. Moving the data from the Climate Data Store to the Google Cloud Platform turned out to be time and resource intensive, and the ingested Earth Engine assets are not modifiable. The example of making C3S data available via the Google Earth Engine shows that we have to work towards the interoperability of different data systems to make data exchange and sharing easier and to make open data more easily accessible to everyone.

Use by the World Food Programme

Earth Engine users welcomed the availability of ERA5 data for their applications. One Earth Engine user who uses ERA5 data is the World Food Programme (WFP). Part of the daily work of WFP's Geospatial Support Unit of the Emergency Division is to monitor 80 countries where it has operations. This requires the use of large volumes of Earth observation data related to the onset of emergencies to provide life-saving humanitarian aid. Weather-related disasters are one of the priorities of the WFP's Emergency Division because they often lead to humanitarian crises and directly affect WFP's operations on the ground. The Geographic Information System unit of WFP uses reanalysis data from ECMWF in Earth Engine to run daily analytics of weather- and climate-related events.

For more information on the Google Earth Engine and access to selected ERA5 data, visit: https://earthengine.google.com/.

For more information on ERA5 and full access to ERA5 data via the Climate Data Store, visit: https://climate.copernicus.eu/climate-reanalysis.

Progress towards assimilating cloud radar and lidar observations

Marta Janisková, Mark Fielding

Successful weather forecasts start from accurate estimates of the current state of the Earth system. Such estimates are obtained by combining model information with Earth system observations in a process called data assimilation. Recent work at ECMWF has demonstrated for the first time that assimilating cloud observations from satellite radar and lidar instruments into a global, operational forecasting system using a 4D-Var data assimilation system is feasible and improves weather forecasts.

Motivation

Cloud-related satellite radiance observations have been at the forefront of recent advances in data assimilation at ECMWF. However, one weakness of these new observations is that they contain limited information on cloud structure, which can lead to ambiguities in the positioning of clouds in the model. Active observations from profiling instruments, such as cloud radar or lidar, contain a wealth of information on the vertical structure of clouds and precipitation but have never been assimilated in global numerical weather prediction (NWP) models. Currently there are no fully functioning space-borne radar or lidar instruments, but historical observations from CloudSat and CALIPSO (Cloud-Aerosol Lidar and Infrared Pathfinder Satellite Observations), part of the NASA A-train constellation, are useful datasets for feasibility studies. In the next few years, new satellite missions with cloud radar and lidar are planned, such as EarthCARE (Earth, Clouds, Aerosols and Radiation Explorer) from the European Space Agency (ESA) and the Japan Aerospace Exploration Agency (JAXA), which has been described by Illingworth et al. (2015).

Previous studies, in particular the STSE Study funded by ESA (Janisková, 2014), have indicated that observations of clouds from space-borne radar and lidar are not only useful to evaluate NWP model performance, but that they also have potential for use in assimilation to improve the initial atmospheric state (the analysis). The studies have demonstrated that a two-step technique which combines one-dimensional (1D-Var) with four-dimensional (4D-Var) data assimilation, where radar reflectivity and attenuated backscatter profiles are indirectly assimilated via pseudo-observations of temperature and humidity, can improve the analysis and forecasts (Janisková, 2015).

Inspired by the success of these previous studies, the ECMWF 4D-Var system has been adapted to enable the direct assimilation of radar and lidar observations. The direct (in-line) data assimilation and monitoring systems were developed during the most recent ESA project on EarthCARE assimilation (Janisková & Fielding, 2018). 4D-Var assimilation experiments have been performed using CloudSat cloud radar reflectivity and CALIPSO lidar backscatter. Using the full system of regularly assimilated observations at ECMWF, several experiments have been carried out in which these observations were added to the system. This is the first time that the feasibility of assimilating such observations directly into a global-scale 4D-Var system has been demonstrated. The results are promising, with improvements in forecast skill shown for temperature, wind and the model radiation budget. Selected results from this encouraging study are presented here.

Prerequisites

To prepare the data assimilation system for the new observations of cloud radar reflectivity and lidar backscatter, several important developments were required. First, there had to be a reasonable representation of the physical processes related to the observations, such as moist processes related to large-scale and convective cloud formation, as well as an 'observation operator' providing realistic model equivalents to the observations (see Box A).

Second, to handle observations appropriately in the data assimilation system, quality control and screening as well as a bias correction scheme are required. The quality control for the cloud radar and lidar observations is based on thresholds for indicators of signal strength; first-guess departures (the differences between observations and the short-range forecasts used in the data assimilation system, called the 'first guess'); estimated total attenuation; and, for radar, expected multiple scattering. The bias correction is based on a climatology of first-guess departures, covering a period when the observations were passively monitored. To provide an implicit regime dependence, the bias correction depends on temperature and height. Another important component of the system is the

doi: 10.21957/72xdt8mj03

a The observation operator

A prerequisite for the assimilation of any type of observation is that the model must be able to simulate the observations with a sufficient degree of realism. For remote-sensing observations of clouds, this means that the model must be able to represent the physical properties of clouds (e.g. their water content) and their appearance as seen from a particular remote-sensing instrument. In the case of height-resolved measurements, the model must also be sufficiently accurate in assigning the correct (or close enough) altitude to clouds.

The observation operators used for CloudSat and CALIPSO are similar and follow the same overall method. For each radar or lidar profile, the nearest model profile is used as input to a look-up table that contains pre-computed scattering and extinction properties according to hydrometeor mass, type and temperature. These scattering properties are then used as input to a radiative transfer calculation to obtain the model equivalent radar reflectivity or lidar attenuated backscatter. Optional features include the simulation of multiple scattering (where after their first scattering event, photons either remain within the instrument field-of-view or return to it at a subsequent scattering event) and the representation of the sub-grid variability of clouds.

As an example, the figure shown below shows the performance of the observation operators for an A-train track on 15 September 2009 over the Pacific Ocean and Japan that includes a direct overpass of Typhoon Choi-wan including its eyewall. The overall performance of the model is very good: many of the cloud features shown by the observations are present in the model equivalents. The figure also shows how the lidar provides mostly information on ice cloud and liquid cloud top height as the signal attenuates very quickly. The radar provides more information on vertical structure and is only completely attenuated in deep convection, such as in the rain bands close to the typhoon eyewall.

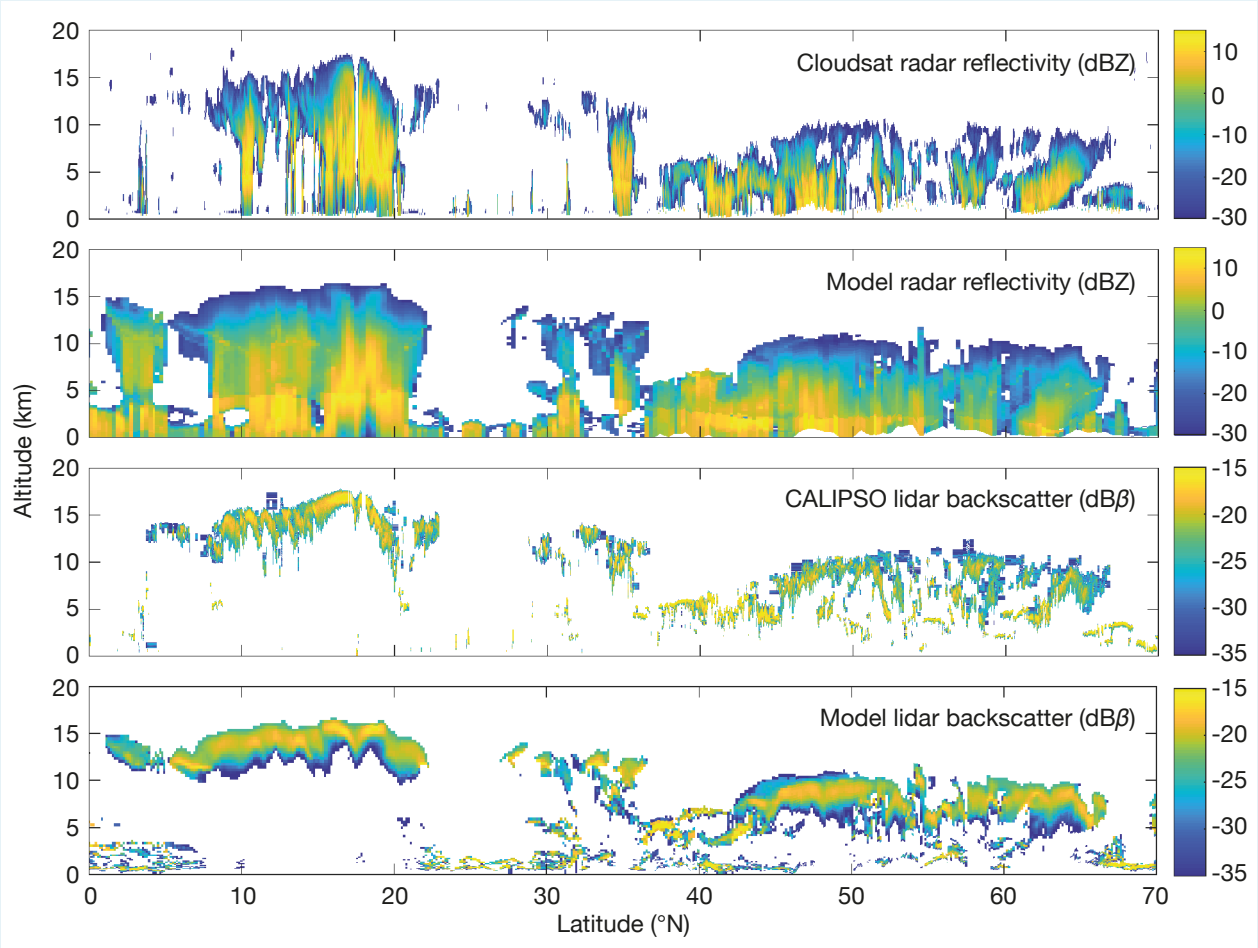

CloudSat radar observations and model equivalents on 15 September 2009 over the Pacific Ocean and Japan (top two panels) and corresponding CALIPSO lidar observations and model equivalents (bottom two panels).

definition of the errors assigned to observations. The assumed observation errors take into account instrument errors, observation operator errors, and representativeness errors due to the narrow field of view, as described in Box B.

Experimental setup

In our study, measurements of cloud radar reflectivity from the CloudSat 94 GHz radar and of lidar backscatter due to clouds at 532 nm from CALIPSO have been assimilated in the 4D-Var system. Using the full system of regularly assimilated observations at ECMWF, several assimilation experiments have been performed using ECMWF's 4D-Var data assimilation system for the three-month period from 1 August 2007 to 31 October 2007, at a horizontal resolution of TCo639 (corresponding to a grid spacing of approximately 18 km on a cubic octahedral grid) and 137 vertical levels.

Many different experiments have been performed to understand the new observation type, such as using different combinations of observations (radar only; lidar only; or both observations in combination with all other assimilated observations), different observation errors (different degrees of error inflation) or observation reduction (increased horizontal averaging or vertical thinning). Here, we present the results from only one of the experiments. In that experiment (EXP), on top of all other normally assimilated observations, both cloud radar reflectivity and lidar backscatter were assimilated using double observation errors compared to the ones estimated in Janisková & Fielding (2018), also described in Box B, and applying observation reduction by horizontal averaging of cloud radar and lidar observations to the coarser resolution of 72 km. For comparison, a control experiment (CTR) was carried out with all regularly assimilated observations, but without the new cloud radar and lidar observations included in the 4D-Var system. Ten-day forecasts were run from the analyses to study the impact of the new observations not only on the analysis but also on forecasts.

Results

The first step in evaluating the impact of assimilating cloud radar reflectivity and lidar backscatter is to compare the resulting analysis against these observations. This evaluation showed that the analysis is closer to cloud radar and lidar observations than would be the case if these observations were not assimilated. The fact that the analysis is drawn to the radar and lidar observations can be seen in Figure 1, where the impact of observations of individual clouds can be assessed. For example, in the analysis, both the structure of the precipitation within the warm front of the North Sea cyclone and the ice cloud in the Atlantic Cyclone south of Greenland are brought closer to the observations.

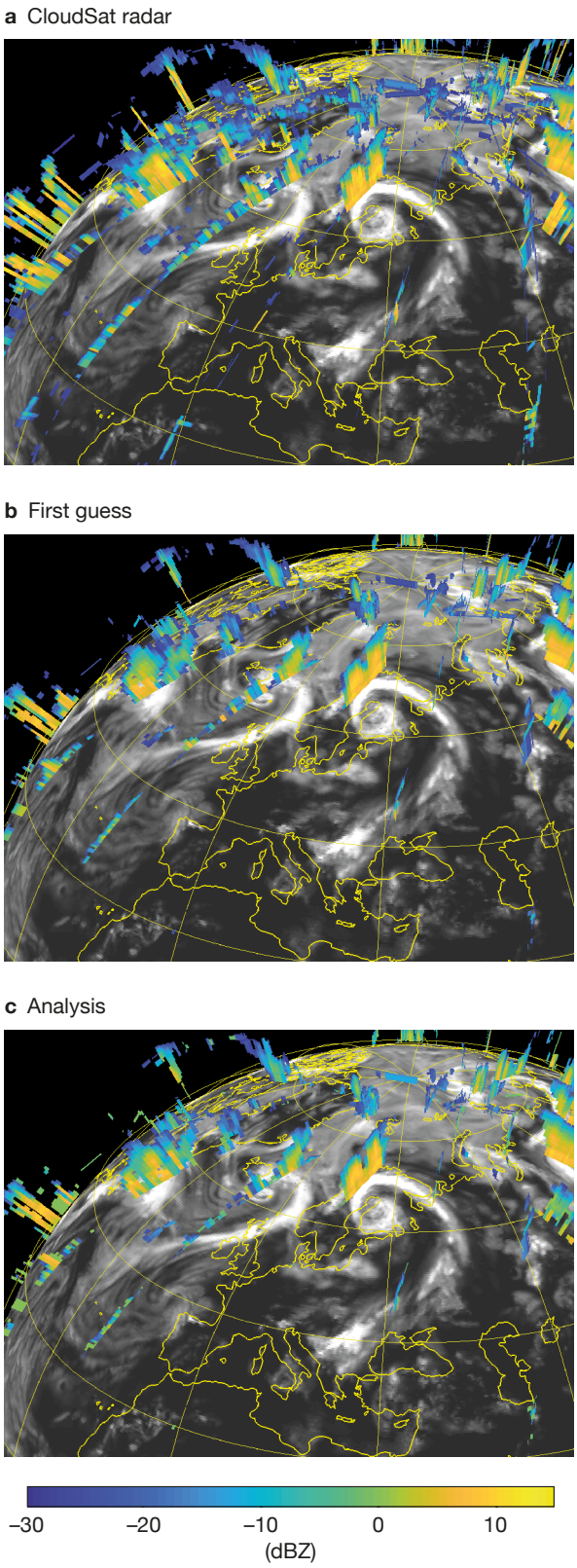

FIGURE 1 Cross sections of radar reflectivity corresponding to various portions of orbital track inside a 12-hour assimilation window for the 00 UTC analysis on 1 August 2007. The panels show (a) observed CloudSat radar reflectivity (dBZ), (b) model equivalent first-guess radar reflectivity using the model background (dBZ) and (c) model equivalent analysis radar reflectivity using the model analysis from the assimilation experiment using all observations including radar and lidar. Note that the first-guess and analysis radar reflectivity is only shown where hydrometeors are detected in both the model and observations.

b Observation errors

In addition to the observations, a key input into a data assimilation system is the estimated error of the observations. The observation error, in combination with the error in the short-range forecasts used in the data assimilation system, controls the weight of the observations in producing the analysis. In 4D-Var, the observations are assumed to be unbiased and their random error is assumed to be normally distributed. At ECMWF, many observations are assigned a static error based on the instrument error and/or first-guess departure statistics. For profiling observations of clouds, the observation error tends to be much more situation dependent and warrants a more complex approach.

To characterise the observation error for the radar and lidar observations, we take an 'error inventory' approach, where individual components of the observation error are specified before being squared and added together (assuming no correlation). The three main sources of error accounted for are instrument error, observation operator error and representativeness error. The figure below provides a breakdown of the different sources of observation error for the same CloudSat A-train track as in Box A. In this figure, the observed radar reflectivity has been averaged to a grid spacing of about 18 km. However, in the experiments presented in this article we used a coarser grid spacing of about 72 km.

For the radar observations, the greatest source of error is the representativeness error, which accounts for the mismatch of scales between the narrow footprint of the observations and the model. To quantify the error, we combine the along-track variability in the observations with a climatological correlation function (Fielding & Stiller, 2019). The greatest representativeness error tends to be found in convective situations; note the increase in error around the typhoon's eyewall at 17°N. The second largest source of error is the observation operator error. This is computed using a Monte Carlo approach, by perturbing the microphysical assumptions (such as particle size distribution and particle scattering properties) in the observation operator. The smallest errors tend to be in the middle of clouds and the largest in regions of strong attenuation. Finally, the smallest component of the overall error is the instrument error, which is calculated dynamically using the instrument signal-to-noise ratio. Away from cloud edges, the instrument error tends to be dwarfed by the other errors.

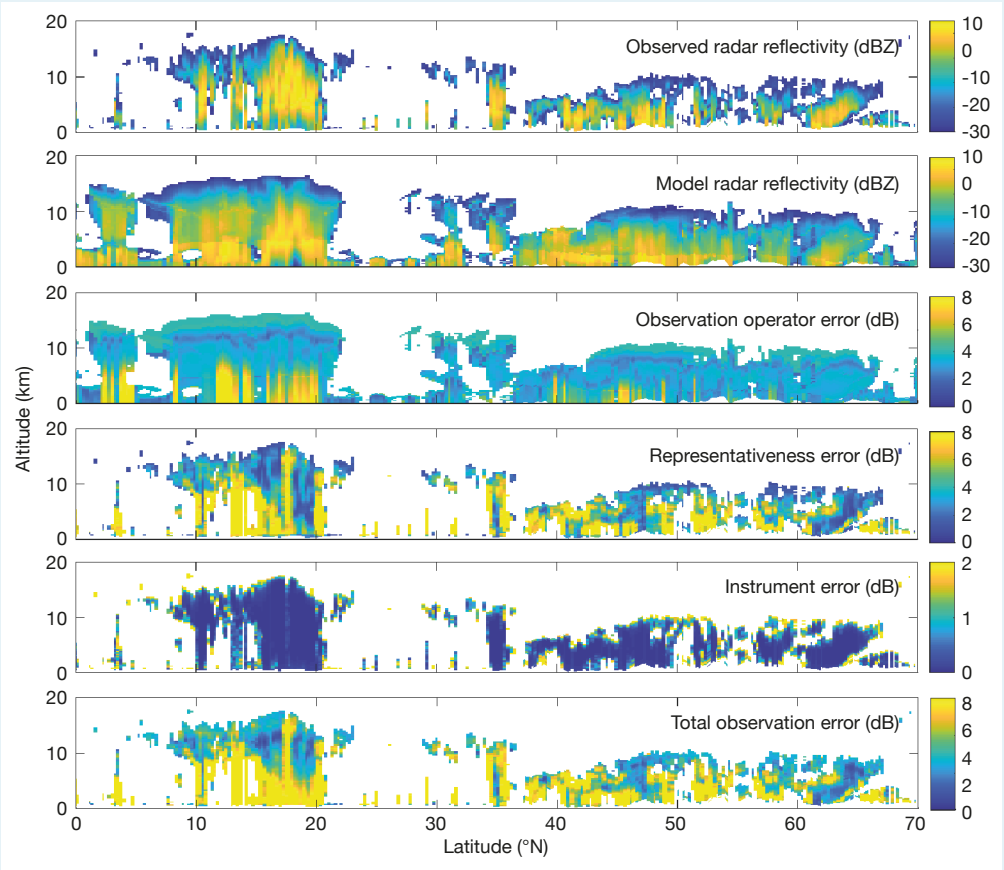

CloudSat radar observations and model equivalents on 15 September 2009 over the Pacific Ocean and Japan (top two panels) and associated observation errors: observation operator error, representativeness error, instrument error, and the total observation error (bottom four panels). Note the different scales in the error panels.

Figure 2 compares first-guess departures with analysis departures (the differences between observations and the analysis) with respect to CloudSat cloud radar reflectivity (Figure 2a) and CALIPSO cloud lidar backscatter (Figure 2b). The plots confirm that EXP produces an analysis that is closer to cloud radar and lidar observations than the first-guess. The results also indicate that the analysis is drawn less strongly to cloud lidar observations than to cloud radar observations, perhaps due to the stronger attenuation of the lidar signal, which can lead to ambiguities in the true cloud amount. Investigations are planned to assess whether assimilating the whole profile rather than just when there is cloud in both the model and the observations might help to solve this deficiency.

The impact of assimilating radar and lidar observations on the analysis has also been assessed by comparing the fit of the first guess to other assimilated observations for the same three-month period (Figure 3). The comparison of the first-guess departures between EXP and CTR indicates a slight improvement with respect to satellite temperature observations as seen for both tropospheric and stratospheric channels of the

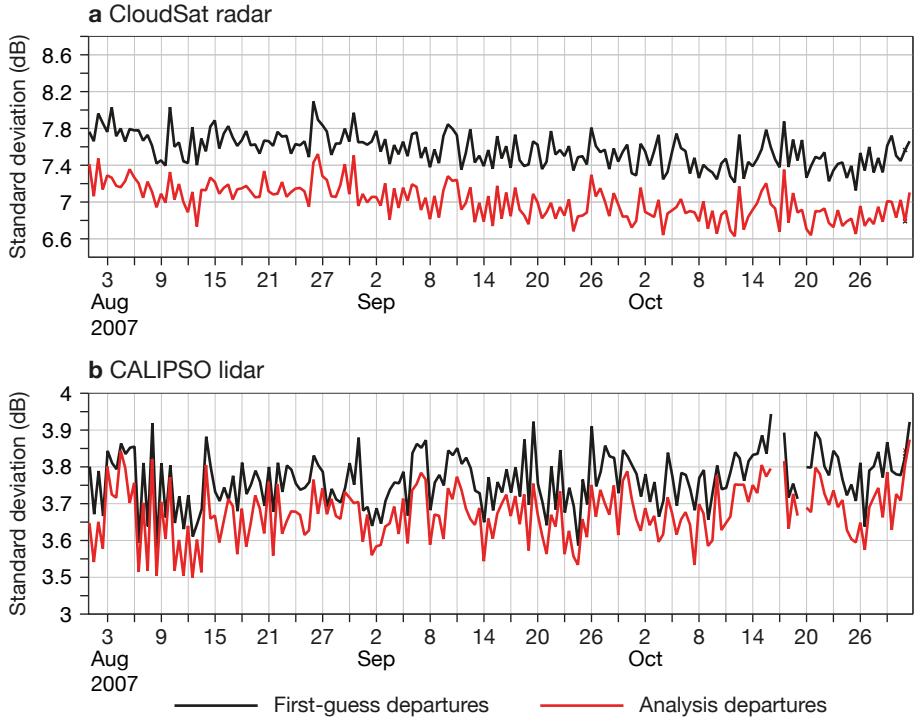

FIGURE 2 Time series of standard deviation for the first guess and analysis departures with respect to (a) CloudSat cloud radar reflectivity and (b) CALIPSO cloud lidar backscatter observations. Results are for the whole globe from the 4D-Var experiment assimilating cloud radar and lidar observations (EXP) for the period from 1 August to 31 October 2007. The standard deviation is a measure of the spread of a distribution, so the standard deviation of departures or errors is a measure of the random component of those departures or errors while filtering out any systematic biases.

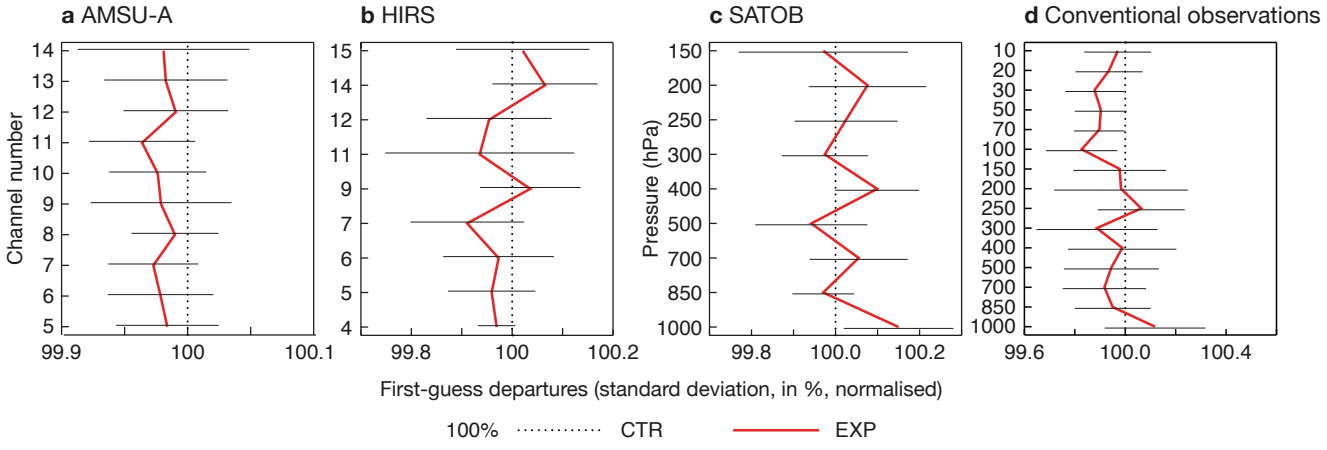

FIGURE 3 Difference in standard deviation between EXP and CTR, normalised by the standard deviation of CTR, for the fit of the first guess to different observations: (a) AMSU-A satellite observations of tropospheric temperature (channels 5–8) and stratospheric temperature (channels 9–14), (b) HIRS satellite observations of temperature (channels 5–8, 13–15) and water vapour (channels 10–12), (c) SATOB wind and (d) wind profiles from conventional observations. The 100% line represents the results for CTR. Horizontal bars indicate 95% confidence intervals. Negative values indicate an improvement in EXT compared to CTR. The results are shown for the whole globe over the period from 1 August to 31 October 2007.

AMSU-A instrument (Figure 3a), as well as for HIRS instrument channels 5–8 and 13–15, which are sensitive to temperature (Figure 3b). An evaluation with respect to wind observations indicates a generally small degradation at around 1,000 hPa, which is more pronounced when comparing the first guess with SATOB wind observations (atmospheric motion vectors). For the levels above, the impact of the new observations on the analysis is broadly neutral when checked against satellite observations, but slightly positive and increasingly better higher up in the troposphere when evaluated with respect to conventional wind observations (such as TEMP, PILOT, AIREP and wind profilers). Overall, verification against other assimilated observations has shown that first-guess departures are either unchanged or slightly reduced when assimilating the new observations.

The impact of the assimilation of cloud radar and lidar observations on the skill of forecasts has been evaluated by verifying forecasts against each experiment's own analysis, as well as against other assimilated and some independent observations (i.e. observations not used by the assimilation system).

Figure 4 shows the impact of assimilating space-borne cloud radar and lidar observations on forecasts up to 10 days ahead over the whole globe for the three-month period from August to October 2007. For temperature, the largest improvement in forecast skill is observed in the lowest levels (especially at 1,000 hPa), while the impact is close to neutral at 850 hPa and above. Similarly, there is a marginally positive impact at 1,000 hPa for relative humidity. Globally, slight improvements in forecast skill for vector wind are most pronounced at the model levels 500 hPa and above. The skill of geopotential forecasts is slightly improved across all levels in EXP. Although one could argue that the overall impact, albeit positive, is rather small, it is important to note that the results presented here are the first ever results of direct 4D-Var assimilation of cloud radar and lidar observations without any extensive tuning. Such tuning is necessary for any new types of observations to be included operationally in the data assimilation system. Therefore, these results are encouraging, but more experiments are needed to further improve the impact of these observations.

A further promising result shows that the model radiation budget can be improved by assimilating cloud radar and lidar observations. This was revealed by verification of the forecast against fully independent observations of the net top-of-atmosphere (TOA) short-wave radiation from CERES (Clouds and the Earth's Radiant Energy System) instruments for the period of August 2007. Figure 5 shows that for EXP the forecast of TOA short-wave radiation is improved up to 60 hours ahead. When looking at day 1 forecasts, there is a positive impact up to 200 km from the A-train track. As expected, the impact diminishes with greater distance from the satellite track.

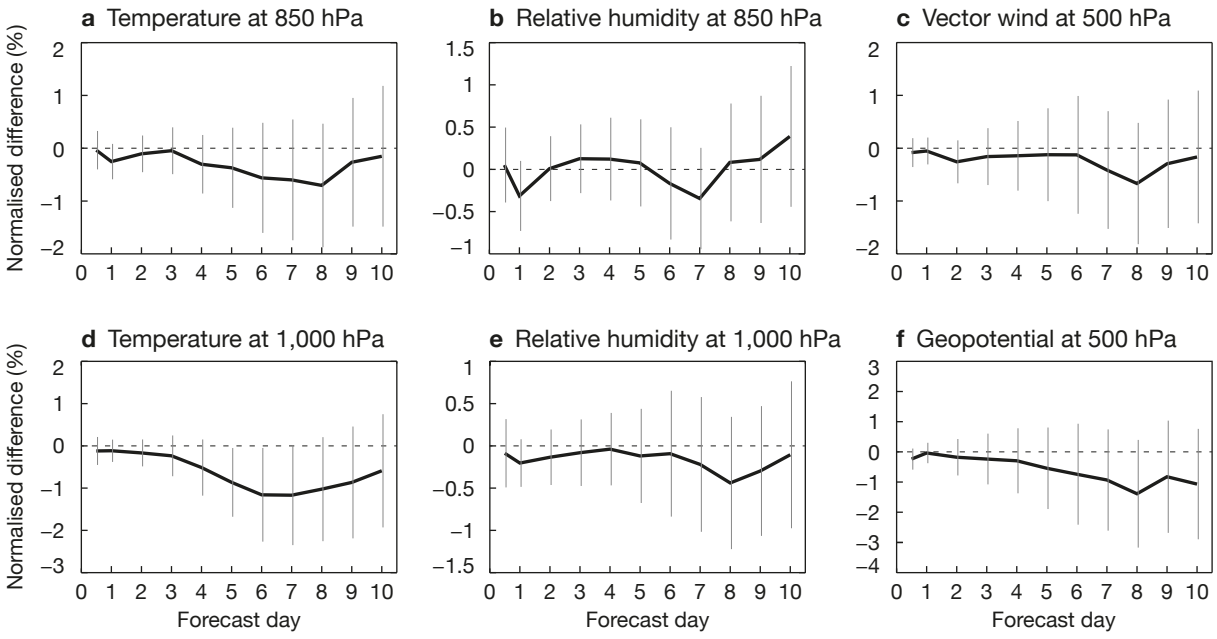

FIGURE 4 Relative impact from the assimilation of space-borne cloud radar and lidar observations (EXP) on forecast scores (root-mean-square error) computed against own analysis, up to 10 days ahead. The score change has been normalised by CTR (the zero line). Bars indicate 95% confidence intervals. Negative values imply a reduction in forecast errors. The scores are shown for (a) temperature at 850 hPa, (b) relative humidity at 850 hPa, (c) vector wind at 500 hPa, (d) temperature at 1,000 hPa, (e) relative humidity at 1,000 hPa, and (f) geopotential at 500 hPa. All scores have been computed over the whole globe for the period of August to October 2007.

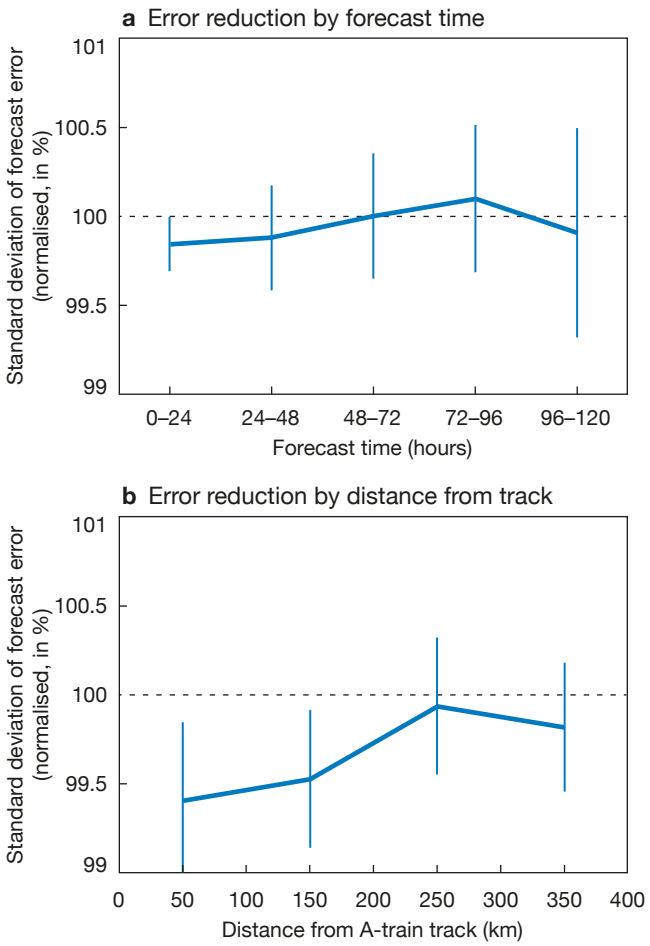

FIGURE 5 Standard deviation of error for EXP forecasts of net top of atmosphere (TOA) short-wave radiation compared to CERES observations for August 2007. The standard deviation of error has been normalised by that of CTR forecasts (the 100% line) so that parts of the plot under the 100% line indicate a reduction in error compared to CTR. Results are shown for (a) different forecast times and (b) different distances from the A-train track for the day 1 forecast. The vertical bars indicate 95% confidence intervals.

Summary and prospects

The assimilation studies presented in this article have demonstrated the potential benefits of assimilating space-borne radar and lidar observations for NWP. The experiments, which cover a period of three months, have shown promising results. Firstly, ECMWF's 4D-Var system provides analyses closer to cloud radar and lidar observations than would be the case if these observations were not assimilated. Secondly, including cloud radar reflectivity and lidar backscatter observations in the 4D-Var system was found to have a positive impact on both the analysis fit to other observations and the subsequent forecast. Increasing forecast skill by including new observations in a well-established observing system is extremely difficult, so these encouraging results warrant further research to maximise the direct benefit of cloud radar and lidar assimilation.

The results presented were found to be sensitive to observation error. As a result, it is envisaged that further gains in forecast skill could be achieved through careful tuning. The correlation of observation error, particularly in the vertical, should also be considered. The behaviour of the assimilation system for different regimes, for example the effect of cloud radar and lidar in convective situations, requires further work and could benefit from improvements in the observation operator assumptions or screening criteria. Another line of potentially very fruitful research is to investigate how cloud radar and lidar observations can support the assimilation of other observation types sensitive to clouds, in particular in the all-sky radiance assimilation framework used operationally at ECMWF. By assimilating the vertical profile of clouds, ambiguity in the height and depth of clouds could be removed, which could improve the impact of the radiance observations.

Further reading

Fielding M. & **O. Stiller**, 2019: Characterizing the representativity error of cloud profiling observations for data assimilation. *J. Geophys. Res. - Atmospheres*, **124**, 4086–4103.

Illingworth, **A.**, **H.W. Barker**, **A. Beljaars**, **M. Ceccaldi**, **H. Chepfer**, **N. Clerbaux**, **J. Cole**, **J. Delanoë**, **C. Domenech**, **D.P. Donovan**, **S. Fukuda**, **M. Hirakata**, **R.J. Hogan**, **A. Huenerbein**, **P. Kollias**, **T. Kubota**, **T. Nakajima**, **T.Y. Nakajima**, **T. Nishizawa**, **Y. Ohno**, **H. Okamoto**, **R. Oki**, **K. Sato**, **M. Satoh**, **M.W. Shephard**, **A. Velázquez-Blázquez**, **U. Wandinger**, **T. Wehr** & **G.J. van Zadelhoff**, 2015: The EarthCARE Satellite: The Next Step Forward in Global Measurements of Clouds, Aerosols, Precipitation, and Radiation. *Bull. Am. Meteorol. Soc.*, **96** (8), 1311–1332, doi:10.1175/BAMS-D-12-00227.1.

Janisková, **M.**, 2014: WP-3200 report: Assimilation experiments for radar and lidar – Support-to-Science-Element (STSE) Study EarthCARE Assimilation, *ECMWF Contract Report to the European Space Agency*.

Janisková, **M.**, 2015: Assimilation of cloud information from space-borne radar and lidar: Experimental study using 1D+4D-Var technique. *Q. J. R. Meteorol. Soc.*, **141**, 2708–2725, doi:10.1002/qj.2558.

Janisková, **M.** & **M. Fielding**, 2018: Operational Assimilation of Space-borne radar and Lidar Cloud Profile Observations for Numerical Weather Prediction, *ECMWF Contract Report to the European Space Agency*.

Recent developments in the automatic checking of Earth system observations

Mohamed Dahoui, Niels Bormann, Lars Isaksen, Tony McNally

For the last few years, an automatic data checking system has been used at ECMWF to monitor the quality and availability of observations processed by the atmospheric data assimilation system (Dahoui et al., 2014). Recently the system has been upgraded to add support for all Earth system observations processed by data assimilation systems running at ECMWF. This includes the 4D-Var system for the atmosphere, land surface data assimilation (LDAS) and ocean data assimilation (OCEAN5). The new framework also makes it easier to cross-check warnings from all components of the observing system and to robustly distinguish between data issues and limitations related to the model and/or data assimilation. Given the increasing size and diversity of the observing system, this tool is playing an essential role in flagging up observation issues and enabling the timely triggering of mitigating actions. On many occasions, the warnings generated by the automatic data checking system have been useful in highlighting unusual events and model or data assimilation limitations. An example is shown in Figure 1. In this article, we describe the most important features of the new system and provide a list of supported observation datasets. The automatic data checking system is partially supported by the EUMETSAT Satellite Application Facility for numerical weather prediction (NWP SAF). The system is chiefly used internally at ECMWF but important notifications are shared with selected users from EUMETSAT and the NWP SAF consortium.

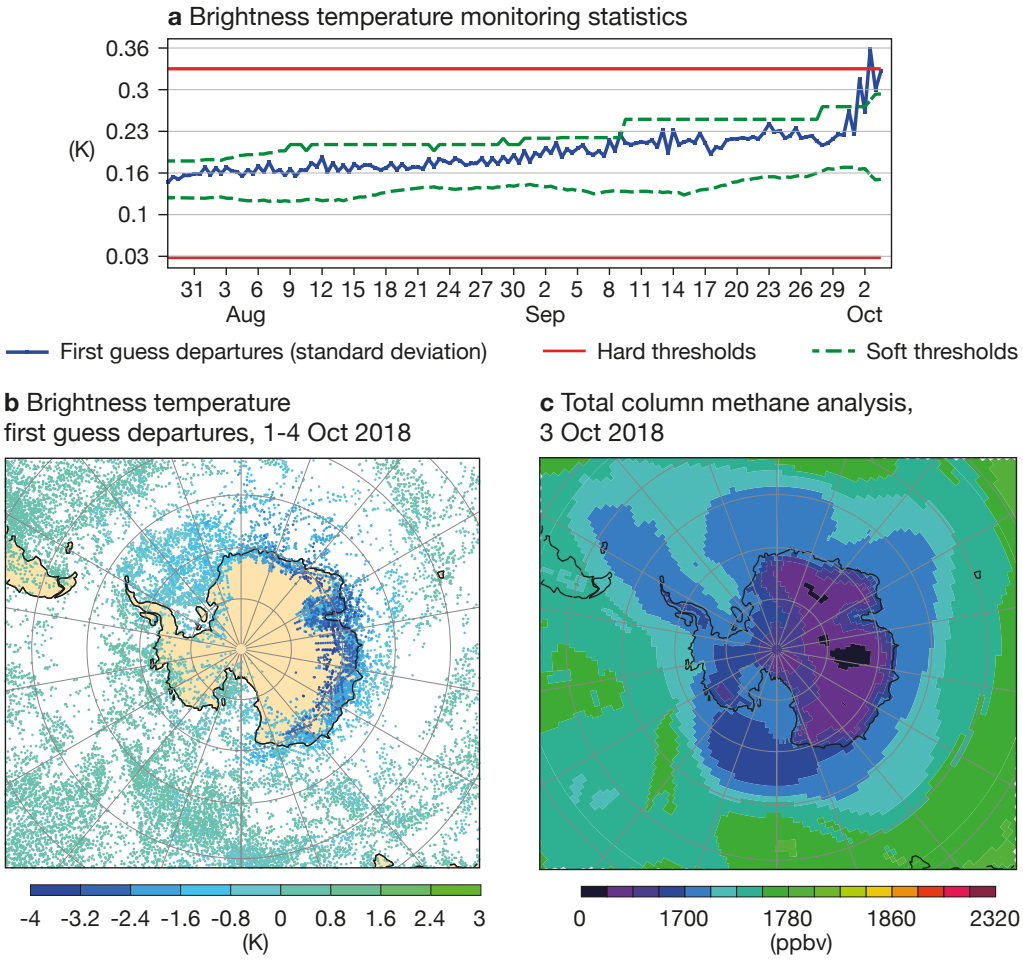

FIGURE 1 These three charts illustrate how the automatic checking system flagged up a case of unusually low concentrations of methane over Antarctica combined with warmer stratospheric conditions. They show (a) a time series of the standard deviation of first guess departures for brightness temperatures from the S-NPP CrIS satellite instrument, channel 789 (7.6 microns), (b) a map of first guess departures for the same channel averaged over the period from 1 to 4 October 2018, and (c) the analysis of total column of methane (in ppbv) for 00 UTC on 3 October 2018 provided by the Copernicus Atmosphere Monitoring Service implemented by ECMWF. The large first guess departures are due to low methane concentrations combined with relatively high stratospheric temperatures in Antarctica.

doi: 10.21957/9tys2md61a

Design of the new system

This significant upgrade of the automatic data checking system had three main objectives: to extend support to all Earth system observations (atmosphere, ocean and land surface); to improve the reliability of the system (by reducing the false alarm rate and maximising the detection efficiency); and to modernise the underlying software to enhance modularity and simplify maintenance. The new system is based on a mixture of Python and shell scripting. The modular design of the previous system has been preserved and improved. It is based on four main components: data retrieval; threshold computation; data checking; and warning notifications (see Figure 2). Warnings are archived in an event database that is subsequently used for web publishing and blacklist generation. The system interfaces directly with the ODB (ECMWF Observations Database) for inputs. Intermediate statistics and thresholds are also based on the ODB format. This enables the software to use ECMWF ODB-API tools for encoding and filtered decoding. Most of the settings are controlled by a few configuration files, which makes it easy to maintain the system and to add support for new data types.

Computing the thresholds

Warnings may be issued when the observations are found to cross certain thresholds. There are two types of thresholds: flexible or 'soft' thresholds, which are used to detect sudden changes in the data, and 'hard' thresholds, which are used to detect slow drifts in the data. The computation of soft thresholds is based on the past 10 days, excluding the last two days. Outliers are excluded by default. Experience shows that this is best achieved by keeping data between the 10th and 80th percentiles. The soft thresholds can optionally be dependent on the analysis cycle. This is currently applied to data types for which the diurnal cycle is important, or data availability is time dependent. As in the previous system, the soft thresholds are bound by hard thresholds. The computation of hard thresholds is performed on demand when needed and automatically on a three-monthly basis to adjust to seasonal variability. As in the previous system, hard thresholds are not used for in-situ data, whether from individual stations or area-based statistics. This choice was initially made to simplify the maintenance of the system. However, there are plans to introduce hard thresholds for in-situ data over geographical domains to persist warnings due to soft thresholds being exceeded, as the soft thresholds adjust quickly to persistent changes in the data.

One of the new aspects of the system is the possibility to automatically monitor satellite data over specific geographical areas in addition to the global domain. This has the advantage of distinguishing between data-related issues and model or data assimilation limitations. Problems flagged up over all areas are clearly due to anomalies with the data. Warnings limited to one domain or two neighbouring ones are indicative that the root cause of the deviations is not data related. The new system also monitors selected satellite data over land

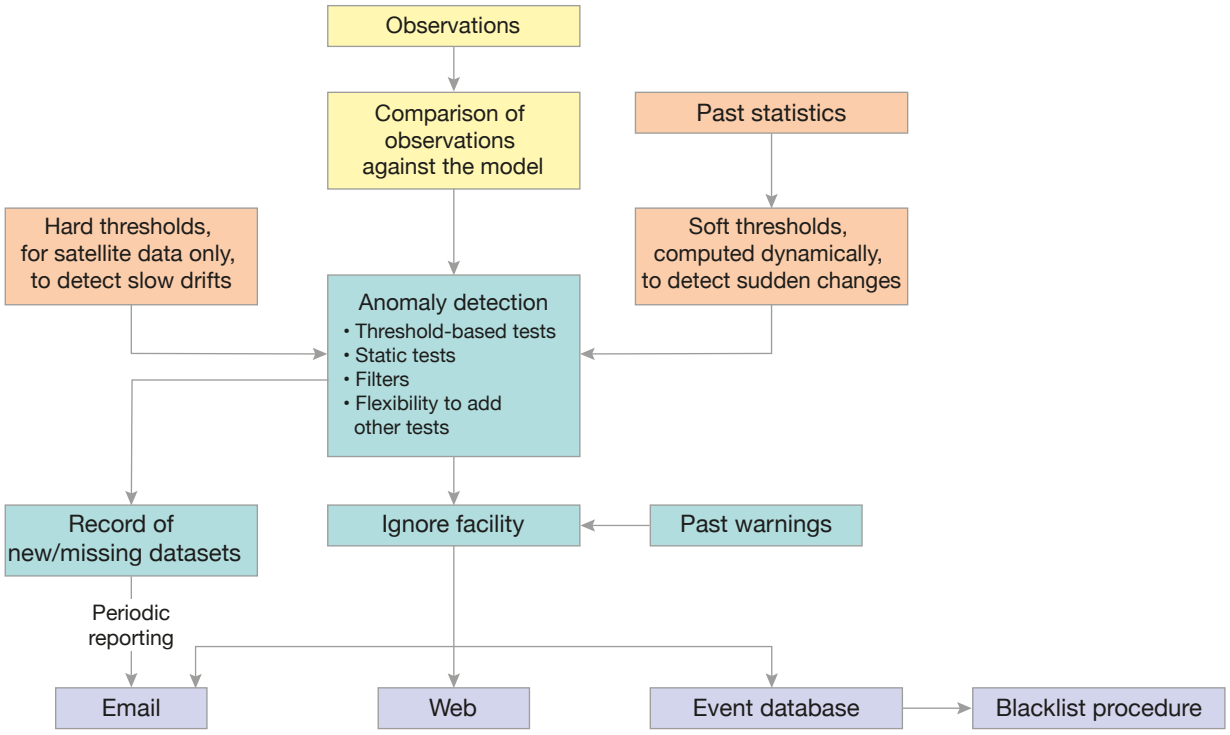

FIGURE 2 High-level diagram of the automatic checking system.

and sea separately in addition to all surface types combined. Currently warnings specific to land or sea areas are ignored pending an improved tuning of filters, to avoid too many insignificant alarms. For all data types, the Ensemble of Data Assimilations (EDA) spread is systematically checked. Doing so helps to distinguish between data issues on the one hand and model or data assimilation issues on the other. Increased EDA spread is usually a sign that large departures between observations and the short-range forecasts used in the data assimilation system (first guess departures) are due to large model uncertainty. For all data apart from satellite observations, the probability of gross error (PGE) is systematically checked in addition to other observation diagnostics (such as first guess departures). PGE is available for all in-situ data used in the atmospheric 4D-Var data assimilation system. For the other data assimilation systems (OCEAN5 and land surface data assimilation), PGE is computed by the automatic checking system using first guess departures and prescribed observation errors. When the root-mean-square of differences between observations and the analysis (analysis departures) is higher than that of first guess departures, a test is performed to check if this is usual behaviour (as is the case for some non-used satellite data) before generating a warning. A test is also performed to assess the magnitude of the analysis departures. A warning is triggered only if the departures are estimated to be large.

For all data types and for all observation quantities involved, the main test is based on the exceedance of computed thresholds. Such a test inevitably generates several small non-persistent deviations that need to be filtered out, given the large number of checked datasets. To make this possible, several additional static tests are added to either consolidate, discard or temporarily ignore insignificant warnings. The tests are designed based on our experience of running the system and they are expected to evolve with time.

Delivering warnings

If the thresholds are exceeded, a severity level is determined by computing the ratio of the difference between the checked statistics and the mean to the difference between these statistics and the closest threshold (upper or lower).

All flagged warnings are processed by an ignore module designed to filter out known issues. In the previous automatic checking system, the ignore module was limited to a static list updated manually. In the new system, three forms of ignore lists are available:

- Manual ignore list: this is updated manually for known issues (e.g. expected outages)
- Static ignore list: this is generated alongside the hard thresholds and reflects the long-term behaviour of the data. Data usually present in only one analysis cycle are not reported as missing for the other analysis cycles (for example in the case of radiosondes reporting once a day). Data persistently present in small numbers or intermittently present are ignored when their counts are below certain values. Data quality warnings are always reported.
- Dynamic ignore list: this is based on recent availability and usage of the data. The list depends on the analysis cycle. Warnings related to recently blacklisted or missing data will cease after a few days. If the data are reactivated their quality will be checked and reported.

The system keeps records and reports about new/missing data (even for in-situ data from individual stations). The list is continuously made available to selected users. Time series are generated for all data affected by warnings (even missing datasets). For in-situ data, a map is generated to show the geographic distribution of affected stations. When warnings are generated, a module processes them to reduce where possible the number of events to be communicated to users and to alter the severity levels in certain conditions:

- If warnings are generated for the global domain and other geographical domains, then only global warnings are retained.
- If warnings are affecting all surface types as well as sea and land separately, then only warnings affecting all surface types are retained.
- If the same warnings are affecting many channels, then only one message is retained with an indication of the number of channels affected.
- Warnings are ranked by their severity.
- ‘Severe’ warnings are escalated to ‘severely persistent’ if the same warning occurred more than six times during the past ten days.
- Some warnings are ignored because they are not severe enough, but if they are persistent then the system will eventually communicate them to users. This approach helps to limit the number of warnings communicated every day, especially for individual in-situ stations.

The delivery of warnings also depends on the choices made by users of the system. Users can for example specify data types of interest and the severity levels to be applied for warnings to be delivered to them. For most users, the best option is to receive severe warnings only.

Supported data types

Adding support for new observation types is relatively simple. Raw sea-surface temperature (SST) and sea ice data from the UK Met Office's OSTIA product (i.e. data as received) are checked differently from other observations. The check is based on day-to-day variability in the OSTIA fields themselves instead of differences between those fields and the model. Observations supported by the system are summarised in Table 1.

Ongoing developments

Given that most of the checking tests are based on first guess departures, and considering model limitations and the effects of atmospheric variability, the warnings that are generated are not necessarily related to observation problems. This means that, in principle, the automatic checking system can fulfil two functions. Its main function is, of course, to prevent the data assimilation system from using poor-quality observations. But the system can also help to identify

Data type	Geophysical parameter	Vertical resolution	Geographical domains	Surface types
Radiances (all satellites used)	Clear-sky and all-sky radiances	Channels	Global and 5 large domains	Land; sea; and all surface types combined
Wind (all satellites used)	Wind vector difference	Pressure layers every 300 hPa	Global and 5 large domains	All surface types combined
Surface wind (all satellites used)	Wind vector difference	Surface	Global and 5 large domains	Sea
GPS radio occultation	Bending angles	Every 2 km	Global and 5 large domains	All surface types combined
Ozone (all satellites used)	Ozone	Total column and pressure layers (every 20 hPa)	Global and 5 large domains	All surface types combined
Aircraft, Radiosondes, Pilot sondes and profilers	Wind vector difference, temperature and specific humidity (if available)	Pressure layers with 300 hPa binning	Global and 14 large domains	All surface types combined
SYNOP weather stations, METARs (Meteorological Aerodrome reports), SHIP and Buoys	Surface pressure, 2 m temperature (LDAS) and 2 m humidity (LDAS)	Surface	Global, 16 large domains and all WMO blocks	
NexRad	Precipitation	Surface	Global	Land
SNOW	Snow depth	Surface	Global, 5 large domains and all WMO blocks	Land
ARGO floats, Mooring buoys, CTD devices and XBT thermographs	Salinity and Potential temperature (OCEAN5)	Ocean depth with 100 m binning		Sea
Altimeters	Sea-level anomaly (OCEAN5)	Surface	Global and 14 large domains	Sea
OSTIA sea ice	Sea-ice concentration (OCEAN5)	Surface	North Pole, South Pole, HUDSON, Great Lakes, BALTIC	Sea
OSTIA SST (raw data)	SST	Surface	Large number of small domains	Sea
OSTIA sea-ice (raw data)	Sea-ice concentration	Surface	North Pole, South Pole, HUDSON, Great Lakes, BALTIC	Sea

TABLE 1 List of datasets supported by the automatic checking system.

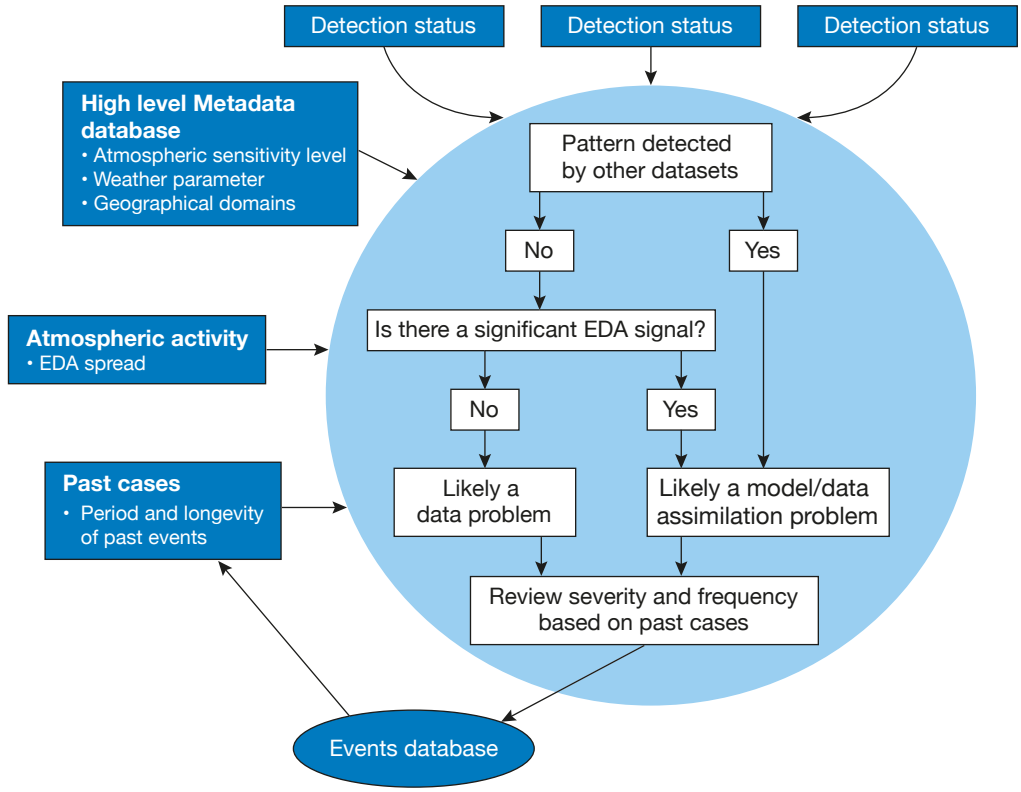

FIGURE 3 Decision tree for the cross-checking of warnings against other datasets.

unusual events and systematic problems in the model or in the data assimilation system. The current implementation of the automatic checking system can partially achieve this objective thanks to the inclusion of the EDA spread and area-based checks. Work is ongoing to exploit redundancies and similarities in the observing system (similar instruments, instruments sensitive to conditions in similar atmospheric layers, etc.) in order to improve the filtering of warnings. For example, a module is being added to cross-check warnings from all components of the observing system against each other using a decision tree algorithm (Figure 3). The system could also exploit information on the past frequency of similar events.

Conclusion

The automatic checking system plays an essential role in protecting the data assimilation system from using poor-quality observations. The recent upgrade of the system has extended support to all Earth system observations used at ECMWF. Further improvements of the system are expected to make it more useful for diagnostic purposes by flagging atmospheric patterns systematically triggering warnings (e.g. onset of sudden stratospheric warming events, orographic gravity waves, mesoscale convective systems, etc.).

Further reading

Dahoui, **M.**, **N. Bormann** & **L. Isaksen**, 2014: Automatic checking of observations at ECMWF. *ECMWF Newsletter* **No. 140**, 21–24.

New products for the Global Flood Awareness System

Ervin Zsoter, Shaun Harrigan, Calum Baugh, Christel Prudhomme

On 5 November 2019, the Global Flood Awareness System (GloFAS) was upgraded to version 2.1. The upgrade includes the release of a revised global hydrological reanalysis based on ECMWF's ERA5 atmospheric, land surface and ocean wave reanalysis. The GloFAS reanalysis is freely and openly available to users through the Copernicus Climate Change Service (C3S) Climate Data Store. The upgrade also introduced a new set of river discharge re-forecasts and revised flood thresholds. In addition, new global flood risk assessment products (summary flood extent and flood impact overview), flood summary maps and ancillary web products have been developed to help users to interpret GloFAS forecasts. GloFAS is the flood component of the Copernicus Emergency Management Service (CEMS) Early Warning Service, for which ECMWF is the computational centre. For more details on GloFAS, see Box A.

River discharge reanalysis

The GloFAS river discharge reanalysis has been updated based on ERA5 data from 1979 to the present (Figure 1). On 5 November 2019, the river discharge reanalysis was made available to the wider community through the C3S Climate Data Store. The reanalysis covers the entire globe and provides information for every day of the last 40 years. GloFAS-ERA5 contains two streams: a quality-assured component, updated monthly with a 2–3-month latency, using the quality-checked and officially released, consolidated ERA5 data, and a more timely component (GloFAST) based on timely ERA5 data (ERA5T). GloFAST is provided daily with an expected latency of two to five days behind real time. The GloFAS-ERA5 river discharge reanalysis will be an invaluable resource to monitor river discharge in near real time anywhere in the world and to understand variability and changes in hydrological conditions. This is especially important for regions where no or few in-situ observations are available. More details are available in Harrigan et al. (2020).

New re-forecasts and thresholds

New river discharge re-forecasts have been produced covering the period 1998 to 2019 for the 'GloFAS 30-day' product and 1981 to 2017 for the 'GloFAS Seasonal' product. Simulations have been performed for a set of past dates using the same model that is used in the real-time forecasts. The re-forecasts have been initialised from the quality-assured component of the GloFAS-ERA5 river discharge reanalysis. These river discharge re-forecasts provide a long, homogeneous forecast time series, ideal for GloFAS forecast evaluation.

The return period flood thresholds were updated in

a What is GloFAS?

The Global Flood Awareness System (GloFAS) is a forecasting service which aims to provide transboundary early flood guidance over every medium to large river basin in the world, helping national hydro-meteorological services, humanitarian agencies and commercial companies to improve their response to flood-related hazards. GloFAS products are delivered through an interactive web service. GloFAS has been developed in close cooperation between the European Commission's Joint Research Centre (JRC) and ECMWF, with support from humanitarian agencies, national authorities and research institutions, such as the Red Cross and the University of Reading. GloFAS couples ECMWF's ensemble weather forecasts with the HTESSEL land surface model (the land surface component of ECMWF's Integrated Forecasting System) to produce surface and subsurface runoff, and the LISFLOOD hydrological model (developed at the JRC) to route the runoff into and through the river network. GloFAS has a 30-day component (GloFAS 30-day), which has produced probabilistic flood forecasts up to 30 days ahead semi-operationally since 2011, and a seasonal hydrological outlook system (GloFAS Seasonal), which has provided high- and low-flow anomalies up to 16 weeks ahead since November 2017. GloFAS officially became part of the Copernicus Emergency Management Service (CEMS) in April 2018, since when it has been offering a fully operational, 24/7 service.

doi: 10.21957/k52du48ez9

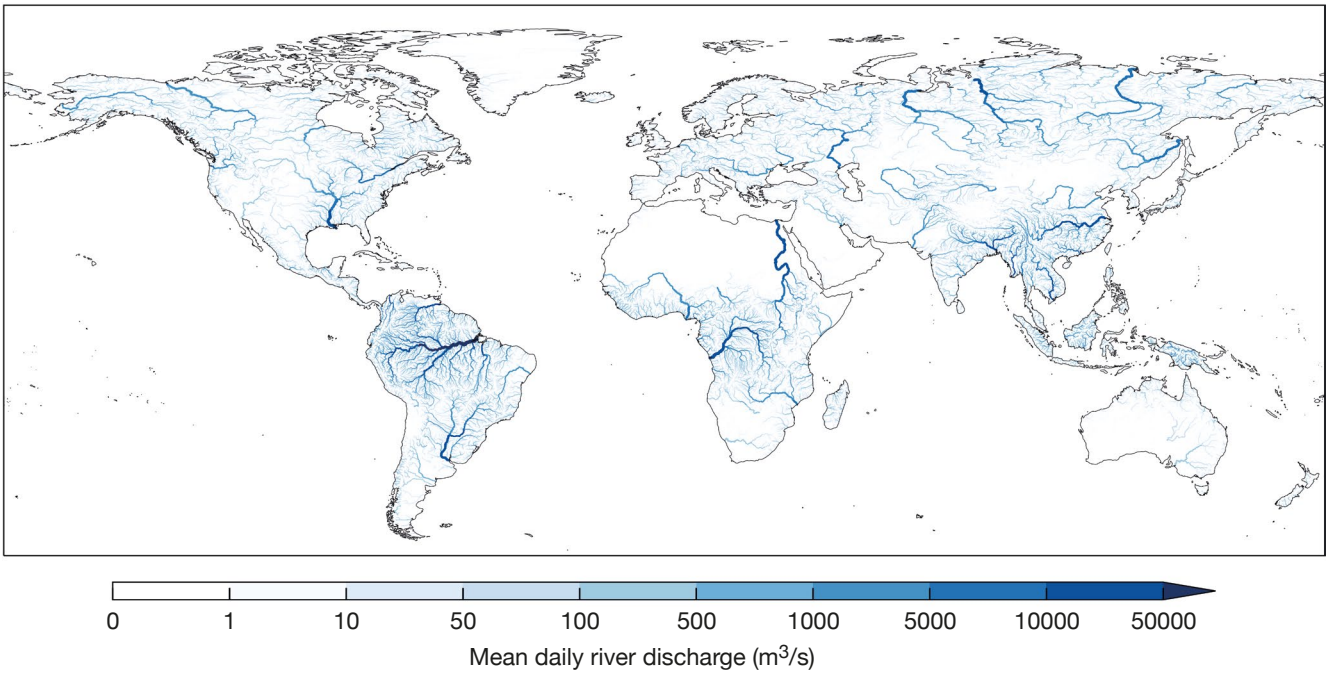

FIGURE 1 Mean daily river discharge from 1979 to 2018 for the GloFAS-ERA5 reanalysis as part of the GloFAS version 2.1 upgrade.

GloFAS 30-day using the GloFAS-ERA5 river discharge reanalysis over the period 1979–2018, while in GloFAS Seasonal the low- and high-flow thresholds were updated using the new seasonal re-forecasts for the period 1981–2017. In addition, there was a small change in the computational methodology for the return period thresholds used in GloFAS 30-day.

Rapid flood risk assessment

GloFAS now includes two global flood impact products: a rapid flood mapping layer and a rapid impact assessment layer (Figure 2). These two products are among the first globally operational products to link streamflow forecasts to predicted inundation area and impact. They are still regarded as

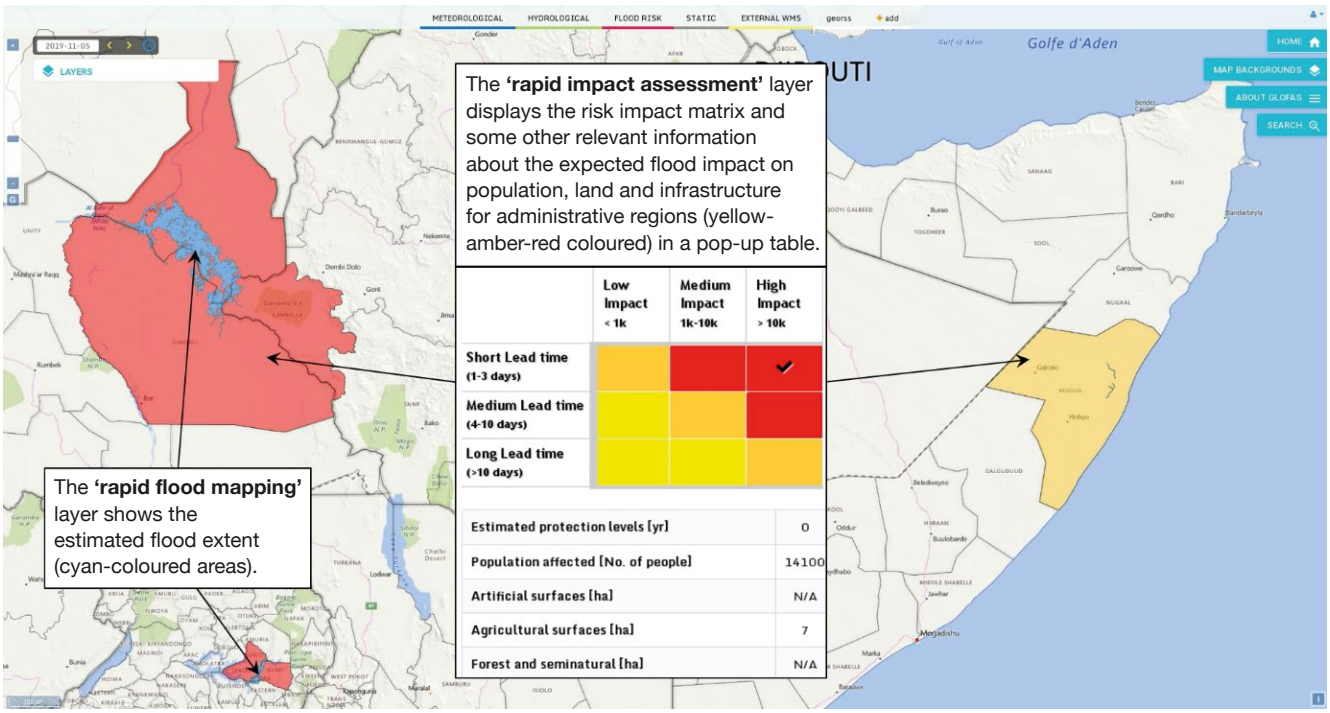

FIGURE 2 Example of the new 'rapid flood mapping' and 'rapid impact assessment' layers. The administrative regions are available in a separate new web layer. These two products are still experimental.

experimental and may evolve over the next few months following user feedback.

The rapid flood mapping layer provides an overview of the estimated flood inundation footprint in river basins with an upstream area larger than 5,000 km^2. Following the methodology already used in the European Flood Awareness System (EFAS), the footprint is defined based on the maximum return period threshold exceeded by the ensemble mean river discharge forecast over the next 30 days. It is extracted from a catalogue of maps for flood events of 10, 20, 50, 100, 200 and 500-year return period magnitudes, pre-generated by the LISFLOOD-FP hydraulic model at a resolution of 0.00833 degrees (corresponding to a grid spacing of about 1 km).

The rapid impact assessment layer shows the potential flood impact on the population and land use, based on the inundated area in the rapid flood mapping layer. Population data is taken from the European Commission's Global Human Settlement Layer (GHSL), and land cover data is taken from the European Space Agency – Climate Change Initiative (ESA-CCI) land cover map series. The total population and areas of land which are exposed to flood hazards are aggregated by administrative region sourced from the Global Administrative Areas database (GADM) and the EU's NUTS (Nomenclature of Territorial Units for Statistics) database in Europe. In the rapid impact assessment layer, the global administrative regions are shaded according to an impact matrix which combines the total population exposure to the flood hazard with the lead time of the flood event. Categories along the top of the matrix refer to the total number of people who live within the flood inundation footprint. If no people live within the footprint, then the rapid impact assessment product is not calculated in that administrative region. The lead time refers to the earliest time of the GloFAS river discharge peak within a given administrative region. Highest impact categories are defined when the flood peak is expected within 3 days, with at least 1,000 people potentially affected by the flood footprint, or for events potentially impacting more than 10,000 people in the next 10 days.

Flood summary maps

Previously, the GloFAS 30-day product summarised flood forecasts in terms of the highest probability across the 30-day forecast horizon for discharge levels to exceed 5- and 20-year return period thresholds. This meant it was difficult for users to identify the timing of the predicted flood wave and its severity across time.

To facilitate a quick diagnostic, a new flood summary map has now been introduced, which combines information on the probability of exceeding all three GloFAS thresholds into a single summary product (Figure 3). It is provided for three forecast periods: short-range (days 1–3), medium-range (days 4–10),

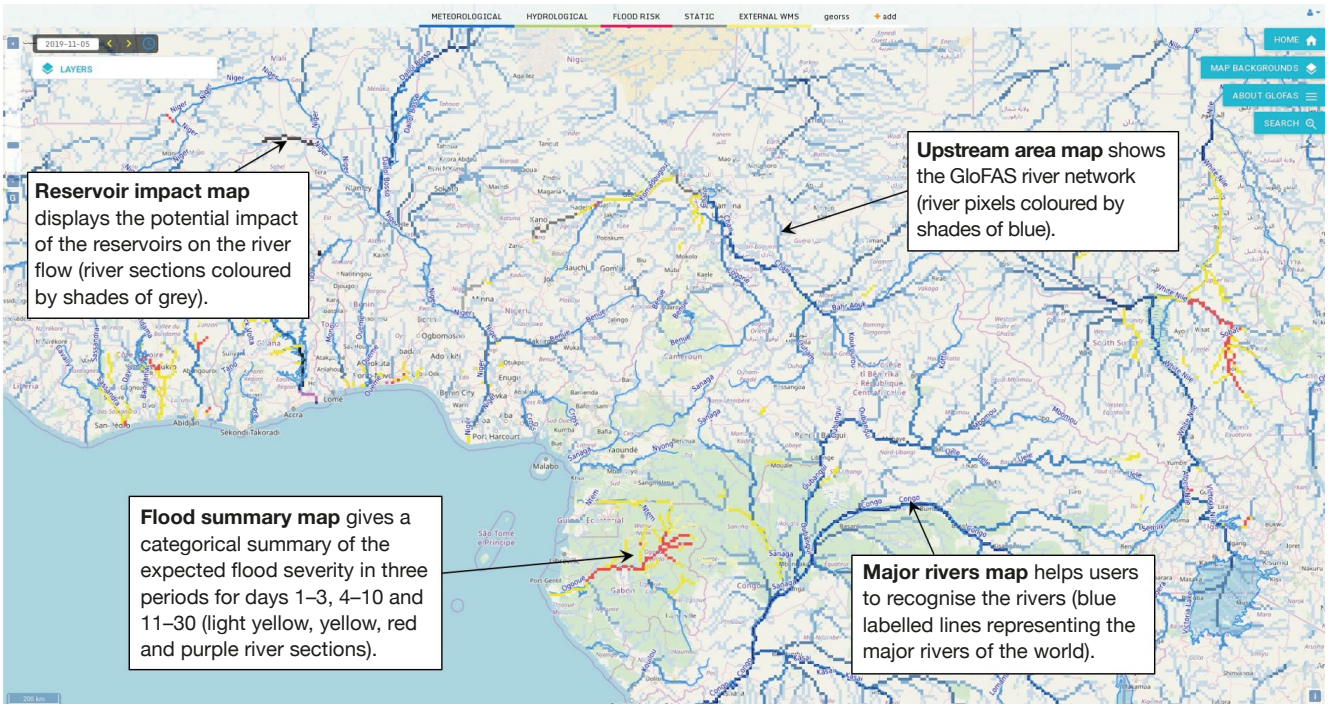

FIGURE 3 Example of new web products. Several new layers were introduced in the GloFAS version 2.1 upgrade that help users to interpret the forecasts. The flood summary maps for three forecast periods, the upstream area map, the reservoir impact map and the map of rivers are available either as standalone layers or can be combined (by overlaying them), as seen in this example.

and extended-range (days 11–30) forecasts. This product is available for all rivers with an upstream area larger than 1,000 km^2. The layers show where the maximum of the ensemble mean river discharge (ENS-max) in the respective forecast periods exceeds the 20-year return period threshold (purple); where ENS-max is between the 5- and 20-year thresholds (red); or where it is between the 2- and 5-year thresholds (dark yellow). In addition, if the probability of exceeding the 2-year return period threshold is greater than 20% (but the ENS-max does not reach the threshold), the river network is coloured in light yellow.

Ancillary maps

Finally, to help users interpret the forecast information provided on the GloFAS website, the following ancillary web products have been added (Figure 3):

- The **upstream area map** shows the catchment area of the GloFAS river network in blue (the darker the colour, the larger the catchment area) for all river basins of more than 1,000 km^2.
- The **reservoir impact map** shows the potential impact of reservoirs included in GloFAS on river discharge at the global scale. It is given as the ratio of reservoir volume to mean annual river discharge at each river pixel.
- The **major rivers map** shows the major rivers of the world along with their name.
- The **administrative regions map** shows the areas used in the new global rapid flood risk assessment product, defined using the NUTS-2 or NUTS-3 classification from EUROSTAT and the region classification from GADM.

Conclusion

This GloFAS upgrade has introduced a range of new products designed to support flood risk assessments at the global level. These include a new global reanalysis of river discharge updated two to five days behind real time, and a range of new products to facilitate flood impact assessments. User feedback on the new products is welcome. More details on the upgrade are available on the GloFAS website (*www.globalfloods.eu*) and on a dedicated ECMWF wiki page (*https://confluence.ecmwf.int/display/COPSRV/GloFAS+v2.1*).

Further reading

Harrigan, **S.**, **E. Zsoter**, **L. Alfieri**, **C. Prudhomme**, **P. Salamon**, **F. Wetterhall**, **C. Barnard**, **H. Cloke** & **F. Pappenberger**, 2020: GloFAS-ERA5 operational global river discharge reanalysis 1979-present, *Earth Syst. Sci. Data Discuss.*, doi: 10.5194/essd-2019-232, under review.

Metview's Python interface opens new possibilities

Iain Russell, Linus Magnusson, Martin Janousek, Sándor Kertész

Metview is ECMWF's interactive and batch processing software for accessing, manipulating and visualising meteorological data. Metview is used extensively both at ECMWF and in the Centre's Member and Co-operating States. A national meteorological service may for example use it to plot fields produced by the ECMWF model and a regional model, calculate some additional fields such as temperature advection, and plot vertical cross sections. The recent addition of a Python interface to Metview has expanded its range of uses and has made it accessible to more potential users. Already, applications in the areas of verification and diagnostics are using the new interface to great effect. The use of Python also opens up new ways of using Metview's functionality, such as through Jupyter notebooks for running data analyses or interacting with training material. For more information on Metview and how to install it, see Box A.

Metview's new Python interface

Python is a scripting language released in 1991. Its popularity has increased greatly in the last few years and it is often taught at universities. This means that Python code can be readily written and understood by many scientists. With the wide use of *NumPy* and several other scientific modules for calculations, the Python environment has become increasingly attractive to scientific programmers. Within this context, it was clear that developing a Python interface to Metview would allow it to be used in conjunction with many other scientific packages, and it would enable more users to start using it without having to learn a new programming language. These potential benefits prompted ECMWF to develop this interface, with the help of the software company B-Open.

The goal of this project was to create a Python module that would provide this interface. The module would give programmers the power of Metview's high-level meteorological data access, manipulation and plotting functions while fully interacting with the rest of the Python ecosystem. To achieve this, some simple

a Metview

Since the release of version 1.0 in 1993, Metview has benefited from constant development work over the years to keep up with the demands of ever-increasing data volumes and more sophisticated ways of interacting with data. In addition to a graphical user interface (GUI), it introduced its own powerful scripting language called Macro. This high-level language allows users to develop concise scripts to process their data and to run those scripts in the operational environment as well as in the research environment. A big advantage of providing a high-level programming language is that Metview developers have been free to change the underlying libraries that Metview uses; for example, the libraries that Metview used for GRIB and BUFR decoding, as well as for data regridding, have been changed in recent years without users having to rewrite any of their code.

Metview is available on ECMWF machines through the *modules* system. Outside ECMWF, it is available in two parts: the binary layer and the Python module. The binary layer can be used as a standalone application through its graphical user interface or its Macro language. One way of installing it is to use the *conda* package manager. From a conda environment on Linux or macOS, the following command will install Metview's binaries: `conda install metview -c conda-forge`. Metview's web pages also provide links to repositories that provide RPM package manager binary installations, and the Ubuntu community maintains a Metview package for their users.

The Python module requires the binary layer to be installed. Available on PyPi, installation is performed simply through the command `pip install metview`. The source code of the Python module is available on github.

doi: 10.21957/hv3sp41ir5

principles were applied: the module should expose all the functionality of Metview's Macro language, but handle native and scientific Python data types where appropriate. Through the use of the *cffi* package, the Python bindings (special code that bridges two programming languages) are able to load a shared C++ library that is installed with Metview and query for a list of available functions. A small translation layer handles the conversion of data types between the C++ and Python code. This system makes it possible for new functions to be added to Metview's C++ code without the need for an update to the Python bindings. It also handles the fact that Python's indexing starts at zero, whereas Metview internally uses 1. Version 1.0.0 of the Python interface was released in December 2018 after much in-house testing of alpha and beta versions.

All of Metview's functions are available in Python through the *metview* namespace, often abbreviated to mv. Figure 1 shows the code required to retrieve 2-metre temperature at different forecast steps and then create a set of time-stamped value averages. The result of the retrieval is a *Fieldset* object, an iterable container with many overridden operators. For example, `t2m_fc - 273.15` would return a new Fieldset with temperatures adjusted to degrees Celsius. Note that most functions can be called in an object-oriented way and a functional way, for example:

```
t2m_fc.valid_date()
```

could also have been written as

```
mv.valid_date(t2m_fc).
```

Providing Metview's functions through a Python module is just one part of making the Python interface work within Python's scientific ecosystem: interoperability with other Python modules requires that data structures can be passed between them. Python has an increasingly well-established set of scientific modules, based around the NumPy module, to efficiently handle data arrays. Metview functions that take vector arguments or return vector results in the Macro language take or return NumPy arrays in Python.

A *Pandas dataframe* is a Python object that contains rows and columns of data, with many methods for analysis and manipulation. Metview's *Geopoints, Odb* and *Table* classes can export their data to a Pandas dataframe with the `to_dataframe()` method. Figure 2 shows some code that filters temperature observation data from a BUFR file, computes the differences between those observations and the model forecast data (read from GRIB), and exports the result to a Pandas dataframe for further analysis.

An *xarray* object presents data as a labelled multi-dimensional hypercube. For meteorological data, the

```
import metview as mv

t2m_fc = mv.retrieve(
    type    = 'fc',
    levtype = 'sfc',
    param   = '2t',
    date    = -5,
    step    = [6,12,18,24],
    grid    = 'o1280')

z = zip(t2m_fc.valid_date(), t2m_fc.average())
for i in z:
    print(i)
```

```
(datetime.datetime(2019, 10, 18, 18, 0), 288.0034532855043)
(datetime.datetime(2019, 10, 19, 0, 0), 287.5664412794946)
(datetime.datetime(2019, 10, 19, 6, 0), 287.9902335998964)
(datetime.datetime(2019, 10, 19, 12, 0), 288.3080870352618)
```

FIGURE 1 Python code using Metview to retrieve and average a time series of forecast fields.

```
import metview as mv

model_t2m = mv.read('t2m_forecast.grib')
obs_bufr = mv.read('obs.bufr')

obs_t2m = mv.obsfilter(
    data   = obs_bufr,
    parameter = 'airTemperatureAt2M',
    output = 'geopoints')

diff = model_t2m - obs_t2m
df = diff.to_dataframe()
print(df.describe())
```

```
          latitude    longitude   level        value
count  1363.000000  1363.000000  1363.0  1363.000000
mean     46.445407    22.170946     0.0    -0.235432
std       8.546075    14.236381     0.0     1.215969
min      30.110000   -22.730000     0.0    -5.261390
25%      40.435000    13.425000     0.0    -0.905671
50%      45.680000    23.110000     0.0    -0.370365
75%      51.550000    32.985000     0.0     0.310031
max      70.930000    45.950000     0.0     6.031244
```

FIGURE 2 Python code using Metview to compute the differences between observations and a forecast field. The result is converted into a Pandas dataframe for further analysis.

dimensions of this hypercube could be latitude, longitude, step and level, for example. In order to map GRIB data into the model used by xarray, a new Python module called *cfgrib* was developed with B-Open. To ensure compatibility with ECMWF data, cfgrib leverages the ecCodes Python module to handle GRIB data. This effort has been very successful, and xarray now officially supports cfgrib as a GRIB engine. Not all GRIB data can be described in such a way. In particular, the geography of non-regular grids, such as reduced Gaussian grids, has no real analogue in xarray, but such grids can still be

considered 1-dimensional data arrays for the purposes of computation.

Metview also uses cfgrib: a Fieldset object has a `to_dataset()` method, which uses cfgrib to generate an xarray dataset from its data. One advantage of this is the convenience with which it is possible to work on specific dimensions of a data cube. Figure 3 shows an example where Metview reads a GRIB file that contains multiple time steps and vertical levels. Then xarray is used to compute the ensemble mean for each level and time step, and the result is passed back to Metview for plotting, with an implicit conversion back to GRIB in the process.

```
import metview as mv

fs = mv.read('wgust_ens.grib')

ds = fs.to_dataset()
ds_mean = ds.mean(dim='number')

mv.plot(ds_mean)
```

FIGURE 3 Using xarray to aggregate on a dimension of the hypercube.

New ways of interacting with Metview

A popular way of interactively presenting and running Python scripts is through a *Jupyter Notebook*, an open source web application for creating and sharing documents containing text, code and graphics. This allows code to be edited and run from within a web browser that is connected to a Python-based server running either on the same machine or remotely. The output, be it text or graphics, can be saved as part of the notebook, allowing others to view it, even if they do not run the code themselves. If the Jupyter server is running locally, Metview's `plot()` command will invoke an interactive plot window. If the command `mv.setoutput('jupyter')` is called, then subsequent plots will appear inline in the notebook, as shown in Figure 4. Jupyter opens new opportunities to interact with Metview and makes it possible to create rich tutorials in the form of notebooks that users can download and run themselves.

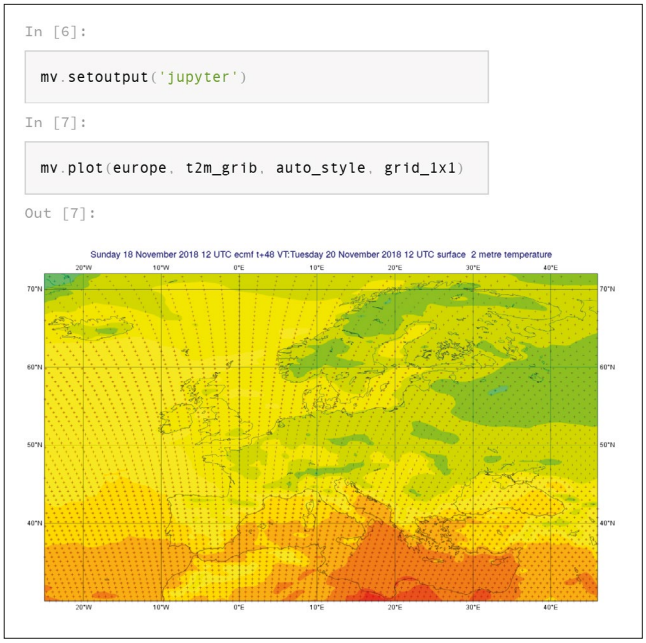

FIGURE 4 Metview's plots can appear inline in a Jupyter notebook.

Use in verification

The availability of Metview's classes and functions in Python has prompted a significant overhaul of a major package in ECMWF's operational verification software. Metview now takes care of all meteorological data decoding, filtering and post-processing, including geography-aware calculations, extending the applicability of the verification software to a wider range of data formats, grids and parameters. Using Metview has significantly reduced the code base of this application and opened up the path to a more modular and fast-to-develop software architecture.

Use in evaluation and diagnostics

For model evaluation and diagnostics, Metview's Python interface is a clear step forward. In many cases, diagnostic work results in a time series of values (or another type of array). Here the combination in Python of using Metview for the calculations on the GRIB files and the Pandas module for making the time-series analysis has proven to be very powerful. One example application is a simple cyclone tracker intended for advanced diagnostics, for which an example of output is shown in Figure 5a. The program is a Python script that uses the Metview module to first retrieve data from the MARS archive. Next, a Python function performs the cyclone tracking by using several Metview functions on the fieldset containing the mean-sea-level-pressure. It returns a new position of the cyclone, which is used together with the `distance()`, `mask()` and `integrate()` functions in Metview to obtain various diagnostic quantities. These are collected in a Pandas dataframe, which can then for example be used for plotting with the matplotlib library. An example is shown in Figure 5b, where various diagnostics for a tropical cyclone are plotted for two high-resolution forecasts (HRES) and two ensemble control forecasts (ENS CF).

Learning about Metview's Python interface

Although the bulk of the Macro documentation has not yet been revised to include Python code, a large amount of work has gone into updating the Metview Gallery so

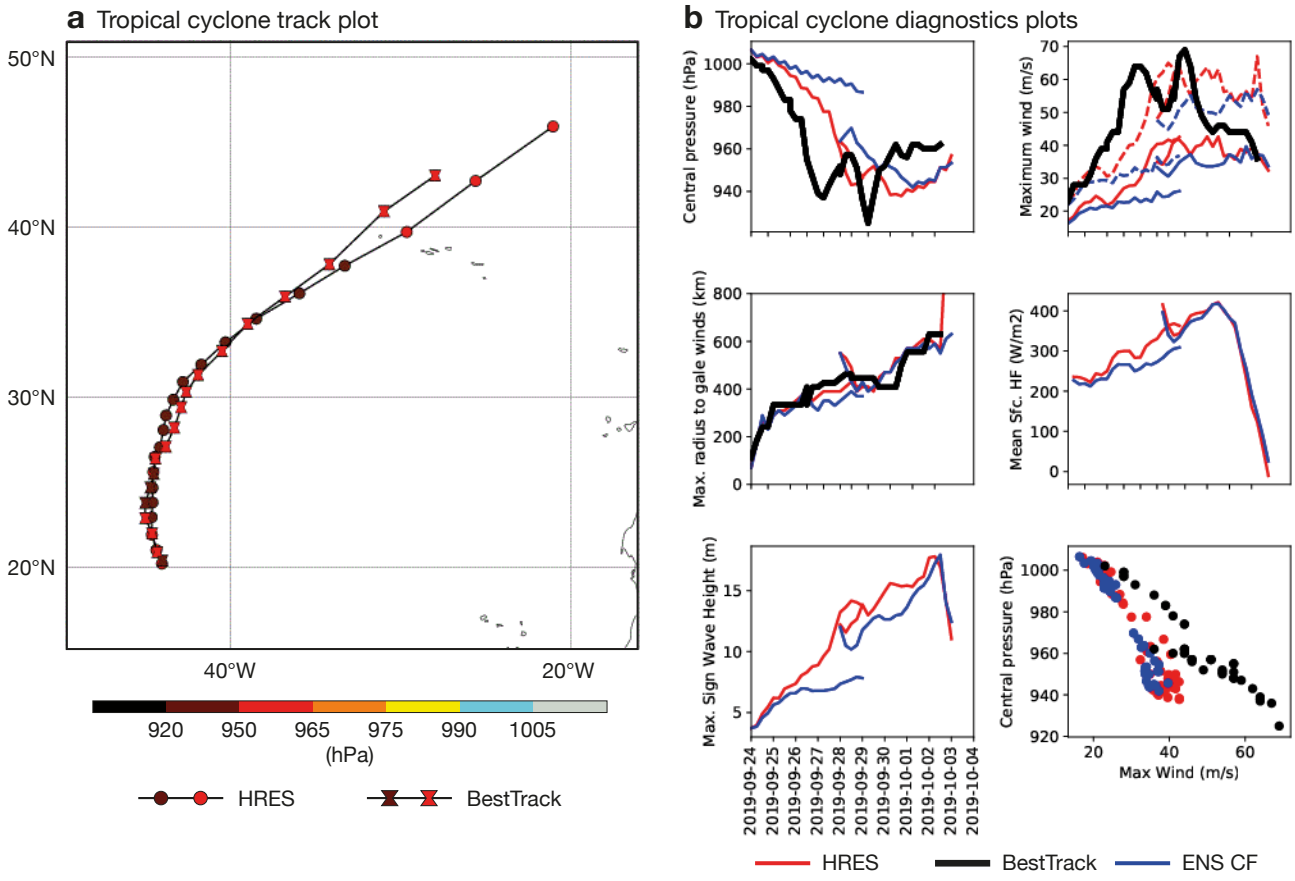

FIGURE 5 Charts computed and plotted in Python with Metview, showing (a) the track of Hurricane Lorenzo in the ECMWF HRES forecast from 28 September 2019 (circles) and the observed track from the BestTrack database (hourglass). The colours of the symbols indicate the central pressure of the cyclone (in hPa). Panel (b) shows diagnostics of central pressure (top-left), maximum wind speed (top-right, solid) and maximum model wind gusts (top-right, dashed), maximum radius to gale winds (middle-left), surface heat flux in the model (middle-right), maximum significant wave height (bottom-left) and wind/presssure relation (bottom-right). The forecasts shown are HRES (red) and ENS control (blue) from 24 and 28 September. The black lines/dots show BestTrack data.

that every example now has a Python version of the code. Also available from the Gallery are a set of Jupyter notebooks with more detailed examples. A number of webinars were given in the last year, and their content is also available from the Metview web pages. Metview's built-in code editor can also help: if running Metview's graphical user interface, many characteristics of computations and plots can be configured interactively and then committed to code by dropping the edited icons into the Code Editor. The editor also provides help with Metview's Python functions by opening the reference web pages at the correct place.

The future

Since Python is a more accessible language than C++, many users will more easily be able to contribute to Metview. Adding new functions to Metview's Python module would be straightforward, but they would not be accessible from the graphical user interface. Work is planned to add the ability to develop Python-based modules that will run alongside the existing C++ modules as part of Metview's service-oriented architecture. This would enable these modules to be run both from the graphical user interface and from Python. In the meantime, Metview's Python interface code is available on github, and we welcome contributions.

Metview's Python interface is a great start in terms of providing high-level meteorological data handling, manipulation and plotting functions to Python, but it is also considered a fundamental building block for future Python work, which could provide higher-level abstractions and further interfacing with established Python modules.

For more information on Metview, visit: *https://confluence.ecmwf.int/metview*.

Metview's Python interface can be found on github: *https://github.com/ecmwf/metview-python*.

Unlocking the hidden value of machine data to improve ECMWF's services

Matthew Manoussakis, Manuel Fuentes, Viktoras Didziulis

"Without data, you're just another person with an opinion." This statement, which is often attributed to the late US engineer and statistician W. Edwards Deming, is no doubt valid in many contexts. Here we set out how machine data generated at ECMWF can help to provide insights that are valuable to the Centre's services.

What are machine data?

Machine data are logs generated by the activity of computers, websites, security systems, networks, smartphones, smart cars etc. They are underused but very valuable as they contain important hidden information. Areas in which they can be useful include: monitoring and troubleshooting, root-cause analysis, performance analysis, security, business analytics, marketing insights, user behaviour and customer support.

Machine data are one of the fastest-growing kinds of big data. Relational databases and traditional methods/software cannot manage these voluminous amounts of data very effectively. As a result, more sophisticated technologies specifically designed for machine logs have emerged and enable organisations to gain new insights from previously inaccessible or untapped data. Moreover, the application of artificial intelligence and machine learning techniques to machine log analytics can help companies to automate some processes and to move from a reactive to a predictive approach in operations.

At ECMWF, one of the main systems that produce large amounts of machine data is MARS, the Centre's Meteorological Archival and Retrieval System. MARS enables users to access ECMWF's meteorological data, e.g. operational forecasts, meteorological observations, reanalyses and many public datasets. Users can access this managed archive from any computer at ECMWF as well as remotely via a web-based application programming interface (Web-API). In a typical day, MARS processes 1.5 million user requests and delivers 400 TB of data.

Analysing the data

MARS and the Web-API produce massive amounts of multi-structured logs on a daily basis, spread out over several systems. Collecting and storing this diverse range of data in a common platform would enable us to analyse the logs more effectively and gain new insights into the entire service.

Two years ago, we decided to work on a proof-of-concept based on Splunk, a log management platform for ingesting, searching, monitoring, and analysing machine logs. Splunk, which had already been used at ECMWF since 2015, can be used to produce interactive tools, reports, alerts, visualisations etc. Initially we worked on historical data to produce relevant reports and

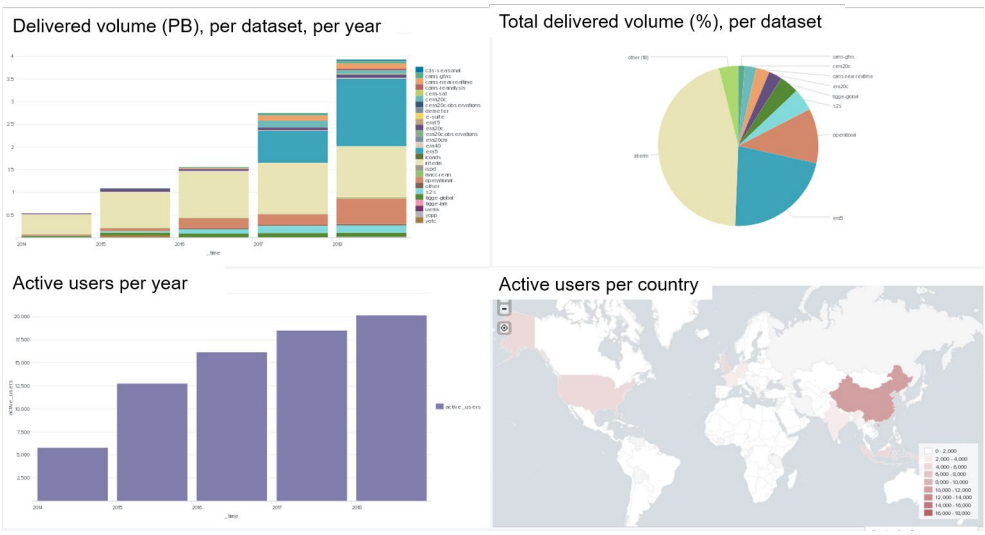

FIGURE 1 Machine data have been used to create these charts showing different aspects of ECMWF Web-API activity from 2014 to 2018, in a customised dashboard.

doi: 10.21957/dc76mm20n3

statistics (Figure 1). We then started to address more day-to-day operational challenges by analysing near-real-time logs (Figure 2). Since then, we have extended the use of Splunk to a wider set of logs and we have automated the logging of different kinds of activity. Some benefits and use cases are presented below.

Operational monitoring and troubleshooting

Speed matters in operational services. By collecting, ingesting and processing live streams of logs in near real time from several systems, we can detect issues, raise alarms early, take immediate action and monitor the health of the operational services more proactively.

FIGURE 2 Near-real-time Web-API user activity by public dataset and location, based on Apache server logs during the previous four hours.

FIGURE 3 A customised dashboard to monitor and troubleshoot Web-API service activity in near real time. A suspicious spike in 'failing' requests can be investigated further by drilling down, through several bespoke dashboards and tools, to the root of the problem and viewing associated events.

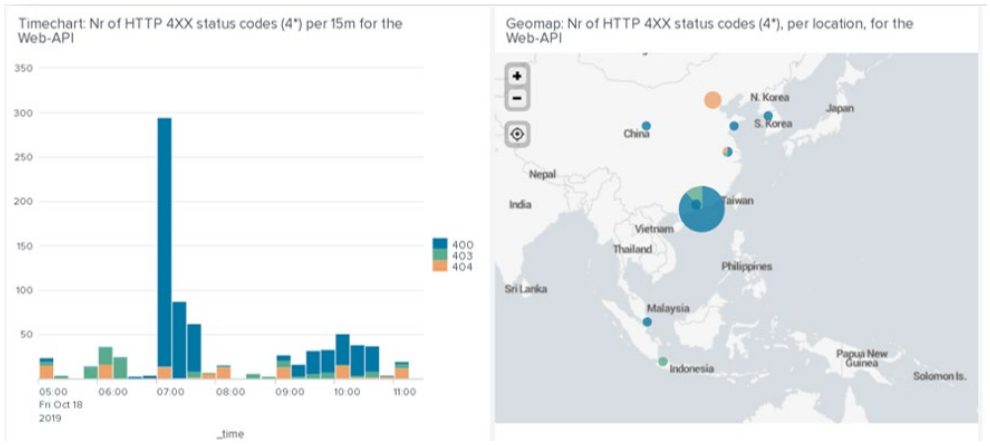

FIGURE 4 An analysis of Apache server logs provides important information on user activity, web traffic and security. In this example, a spike in 4XX HTTP status codes is investigated using predefined tools, including a real-time activity map.

We can combine aggregations of different logs in a single dashboard and correlate patterns across several components in one place. This enables us to have a better overview in near real time.

Through a series of interactive customised dashboards, we can drill down to further investigate an issue (Figures 3 and 4). We can then view associated logs and related charts, isolate and investigate specific problems

and identify anomalies. Previously, it used to take a significant amount of time to collect and analyse this type of information as it had to be gathered from files stored across different systems.

A more data-driven approach

We are developing objective analytics based on historical data to gain smarter insights, obtain optimal answers and make better decisions and plans. For example, we use objective criteria to evaluate the performance of our services using thresholds (Figure 5). These can then be used for purposes such as finding components that are causing poor user experience and managing the lifetime of obsolete datasets. Such objective analysis capabilities have enabled us to identify which datasets are going to be essential to maintain during the migration to our new data centre in Bologna.

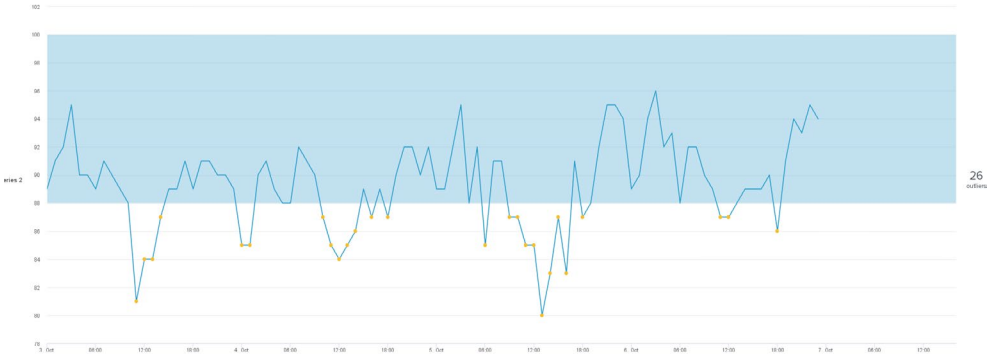

FIGURE 5 The implementation of metrics enables us to increase the performance of our services to a higher sustained level and to improve our users' experience. The chart shows the evolution of elapsed time for Web-API requests. In this example, 26 cases that surpassed a pre-defined threshold were detected during the selected period. If we want to investigate such performance issues, we can simply navigate to the time frame and delve into the logs to see more details about the events.

Communication and collaboration

Sharing our logs within ECMWF has enabled us to better collaborate between teams, and to ensure that we are all measuring the same activity. This helps us to improve our communication and to share insights and knowledge more efficiently. To support the interpretation of the information, we are also developing dashboards customised to the specific needs of different teams (Figure 6).

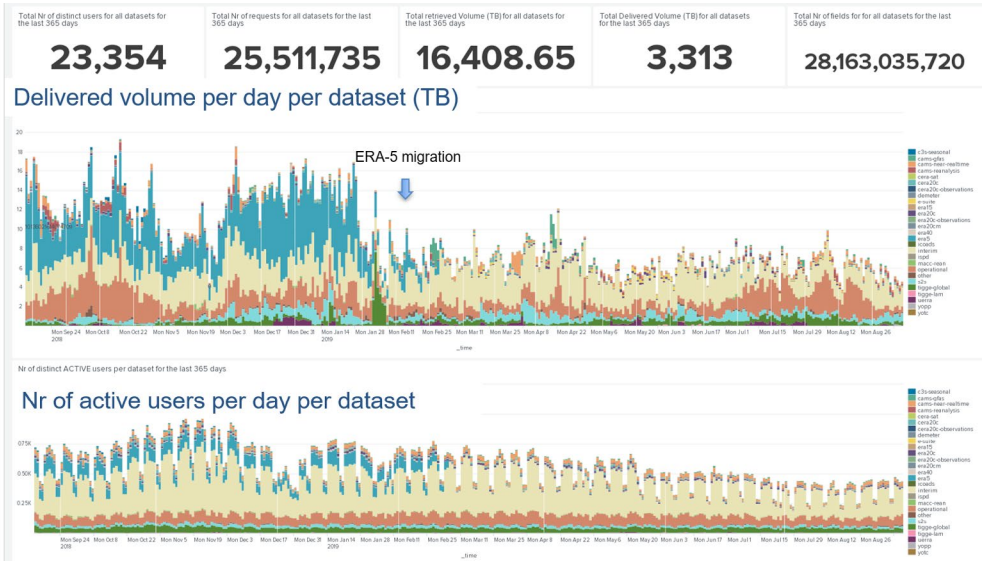

FIGURE 6 Evolution of Web-API activity over 365 days by dataset, in a customised dashboard. This tool enhanced the collaboration between different teams at ECMWF during the migration of users of the ERA5 reanalysis dataset from ECMWF's Web-API to the Climate Data Store (CDS) operated by the EU-funded Copernicus Climate Change Service (C3S) implemented by ECMWF.

Improving DevOps

The project has given us an opportunity to try new ideas that help us to improve our DevOps practices (i.e. practices in which software development and IT operations go hand in hand). One such improvement is the use of tools that enable us to make faster and better decisions about the quality of new Web-API releases. Using a set of dashboards, we can analyse the voluminous logs produced during stress tests, detect any quality or performance issues on new software releases and fix them before the software is deployed in production (Figure 7).

FIGURE 7 A new Web-API release can be checked using interactive bespoke tools that enable us to detect any underlying issues and investigate further.

Conclusions

We have built a proof-of-concept to address the need for a centralised management system for the machine data generated by some of our services. This project is enabling near-real-time monitoring and troubleshooting for the Web-API and it is improving operational visibility across the MARS service. Moreover, it is fostering a more data-driven approach to decision-making and improving communication and collaboration with other teams.

We believe that overall this project has been very successful. It has shown promising results and it has highlighted the importance of a well-defined log management strategy for the effective operation of complex systems.

Looking ahead, we plan to:

- transition this proof-of-concept towards operations
- explore applying the ideas to other services
- investigate artificial intelligence and machine learning concepts and their application to machine data processing
- work to further improve the observability of our services.

Useful links

MARS user documentation: *https://confluence.ecmwf.int/display/UDOC/MARS+user+documentation*

ECMWF's Web-API: *https://confluence.ecmwf.int/display/WEBAPI*

Using Splunk to analyse machine data: *https://www.splunk.com/en_us/resources/machine-data.html*

ECMWF Council and its committees

The following provides some information about the responsibilities of the ECMWF Council and its committees. More details can be found at:

http://www.ecmwf.int/en/about/who-we-are/governance

Council

The Council adopts measures to implement the ECMWF Convention; the responsibilities include admission of new members, authorising the Director-General to negotiate and conclude co-operation agreements, and adopting the annual budget, the scale of financial contributions of the Member States, the Financial Regulations and the Staff Regulations, the long-term strategy and the programme of activities of the Centre.

President Prof. Juhani Damski *(Finland)*

Vice President Gen. Silvio Cau *(Italy)*

Policy Advisory Committee (PAC)

The PAC provides the Council with opinions and recommendations on any matters concerning ECMWF policy submitted to it by the Council, especially those arising out of the four-year programme of activities and the long-term strategy.

Chair Mr Rolf Brennerfelt *(Sweden)*

Vice Chair Mr Eoin Moran *(Ireland)*

Finance Committee (FC)

The FC provides the Council with opinions and recommendations on all administrative and financial matters submitted to the Council and exercises the financial powers delegated to it by the Council.

Chair Mr Mark Hodkinson *(United Kingdom)*

Vice Chair Dr Gisela Seuffert *(Germany)*

Scientific Advisory Committee (SAC)

The SAC provides the Council with opinions and recommendations on the draft programme of activities of the Centre drawn up by the Director-General and on any other matters submitted to it by the Council.
The 12 members of the SAC are appointed in their personal capacity and are selected from among the scientists of the Member States.

Chair Dr Inger-Lise Frogner *(Norway)*

Vice Chair Dr Alain Joly *(France)*

Technical Advisory Committee (TAC)

The TAC provides the Council with advice on the technical and operational aspects of the Centre including the communications network, computer system, operational activities directly affecting Member States, and technical aspects of the four-year programme of activities.

Chair Dr Philippe Steiner *(Switzerland)*

Vice Chair Dr Sarah O'Reilly *(Ireland)*

Advisory Committee for Data Policy (ACDP)

The ACDP provides the Council with opinions and recommendations on matters concerning ECMWF Data Policy and its implementation.

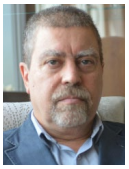

Chair Mr Francisco Pascual Perez *(Spain)*

Vice Chair Mr Paolo Capizzi *(Italy)*

Advisory Committee of Co-operating States (ACCS)

The ACCS provides the Council with opinions and recommendations on the programme of activities of the Centre, and on any matter submitted to it by the Council.

Chair Mr Taimar Ala *(Estonia)*

Vice Chair Mr Nir Stav *(Israel)*

ECMWF publications

(see *www.ecmwf.int/en/research/publications*)

Technical Memoranda

858 **Roberts**, **C.D.**, **A. Weisheimer**, **S. Johnson**, **T. Stockdale**, **M. Alonso-Balmaseda**, **P. Browne**, **A. Dawson**, **M. Leutbecher** & **F. Vitart**: Reduced-resolution ocean configurations for efficient testing with the ECMWF coupled model. *January 2020*

855 **Ingleby**, **B.**, **L. Isaksen** & **T. Kral**: Evaluation and impact of aircraft humidity data in ECMWF's NWP system. *January 2020*

854 **Vitart**, **F.**, **M. Alonso-Balmaseda**, **L. Ferranti**, **A. Benedetti**, **B. Balan-Sarojini**, **S. Tietsche**, **J. Yao**, **M. Janousek**, **G. Balsamo**, **M. Leutbecher**, **P. Bechtold**, **I. Polichtchouk**, **D. Richardson**, **T. Stockdale** & **C.D. Roberts**: Extended-range prediction. *November 2019*

853 **Haiden**, **T.**, **M. Janousek**, **F. Vitart**, **L. Ferranti** & **F. Prates**: Evaluation of ECMWF forecasts, including the 2019 upgrade. *November 2019*

852 **Groenemeijer**, **P.**, **T. Púčik**, **I. Tsonevsky** & **P. Bechtold**: An Overview of Convective Available Potential Energy and Convective Inhibition provided by NWP models for operational forecasting. *November 2019*

ECMWF Calendar 2020

Jan 27–30	Training course: Use and interpretation of ECMWF products (for trainers)
Feb 3–6	Joint JCSDA–ECMWF workshop on assimilating satellite observations of cloud and precipitation into NWP models
Feb 12–13	Workshop on aircraft weather observations and their use
Feb 24–28	Training course: Data assimilation
Mar 2–6	Training course: EUMETSAT/ECMWF satellite data assimilation
Mar 9–13	Training course: Advanced numerical methods for Earth system modelling
Mar 10–12	Workshop on warm conveyor belts as a challenge to forecasting
Mar 16–19	Training course: A hands-on introduction to numerical weather prediction models: understanding and experimenting
Mar 23–27	Training course: Predictability and ensemble forecast systems
Mar 30–Apr 3	Training course: Parametrization of subgrid physical processes
Apr 21-23	Advisory Committee for Data Policy and data policy meetings of ECOMET and EUMETSAT (Denmark)
May 12	Online training: Data manipulation and visualisation – processing and visualising ECMWF ensemble data
May 14	Online training: Data manipulation and visualisation – interactive analysis of ECMWF data
Jun 1–4	Using ECMWF's Forecasts (UEF)
Jun 23–24	Council
Sep 1–4	Annual Seminar: Numerical methods for atmospheric and oceanic modelling – recent advances and future prospects
Sep 14–18	Workshop on HPC in meteorology (Bologna)
Sep 28–30	Workshop on operational measurements for ocean waves
Oct 5–8	ECMWF–ESA workshop on machine learning for Earth observation and prediction
Oct 5–8	Training course: Use and interpretation of ECMWF products
Oct 12–14	Scientific Advisory Committee
Oct 15–16	Technical Advisory Committee
Oct 19–20	Finance Committee
Oct 20	Policy Advisory Committee
Nov 2–5	ECMWF/EUMETSAT NWP SAF workshop on the treatment of random and systematic errors in satellite data assimilation for NWP
Dec 8–9	Council

Contact information

ECMWF, Shinfield Park, Reading, RG2 9AX, UK

Telephone National 0118 949 9000

Telephone International +44 118 949 9000

Fax +44 118 986 9450

ECMWF's public website *www.ecmwf.int/*

E-mail: The e-mail address of an individual at the Centre is firstinitial.lastname@ecmwf.int. For double-barrelled names use a hyphen (e.g. j-n.name-name@ecmwf.int).

For any query, issue or feedback, please contact ECMWF's Service Desk at *servicedesk@ecmwf.int*.

Please specify whether your query is related to forecast products, computing and archiving services, the installation of a software package, access to ECMWF data, or any other issue. The more precise you are, the more quickly we will be able to deal with your query.

ECMWF

Newsletter | **No. 162** | Winter 2019/20

European Centre for Medium-Range Weather Forecasts

www.ecmwf.int